https://doi.org/10.5194/egusphere-2024-2235
Preprint. Discussion started: 7 October 2024

MEASUREMENT REPORT: WINTERTIME AEROSOL CHARACTERIZATION AT AN URBAN TRAFFIC SITE IN HELSINKI FINLAND

Kimmo Teinilä[1], Sanna Saarikoski[1], Henna Lintusaari[2], Teemu Lepistö[2], Petteri Marjanen[2], Minna Aurela[1], Heidi Hellén[1], Toni Tykkä[1], Markus Lampimäki[3], Janne Lampilahti[3], Luis Barreira[1], Timo Mäkelä[1], Leena Kangas[1], Juha Hatakka[1], Sami Harni[1], Joel Kuula[1], Jarkko V. Niemi[4], Harri Portin[4], Jaakko Yli-Ojanperä[5], Ville Niemelä[6], Milja Jäppi[2], Katrianne Lehtipalo[1,3], Joonas Vanhanen[7], Liisa Pirjola[8,3], Hanna E. Manninen[4], Tuukka Petäjä[3], Topi Rönkkö[2] and Hilkka Timonen[1]

[1]Atmospheric Composition Research, Finnish Meteorological Institute, Helsinki, Finland
[2]Aerosol Physics Laboratory, Physics Unit, Faculty of Engineering and Natural Sciences, Tampere University, Tampere, Finland
[3]Institute for Atmospheric and Earth System Research/Physics, Faculty of Science, University of Helsinki, Finland
[4]Helsinki Region Environmental Services Authority (HSY), Helsinki, Finland
[5]Vaisala Oyj, Helsinki, Finland (currently University Association of South Ostrobothnia)
[6]Dekati Ltd, Kangasala, Finland
[7]Airmodus Ltd, Erik Palménin aukio 1, FI-00560 Helsinki, Finland
[8]Department of Automotive and Mechanical Engineering, Metropolia University of Applied Sciences, Vantaa, Finland
Correspondence to: Kimmo Teinilä (kimmo.teinila@fmi.fi)

Abstract. Physical and chemical properties of particulate matter and concentrations of trace gases were measured at an urban site in Helsinki, Finland for five-weeks to investigate the effect of wintertime conditions on pollutants. The measurement took place in a street canyon (Traffic Supersite) in January–February 2022. In addition, measurements were conducted in an urban background station (UB Supersite, SMEAR III, located approx. 0.9 km from the Traffic Supersite) and with a mobile laboratory in the adjacent side streets as well as by driving back and forth along the street along the Traffic Supersite. A source apportionment was performed for the SP-AMS measurements to identify organic factors connected to different particulate sources. Particle number concentration time series and the pollution detection algorithm (PDA) were used to compare local pollution level differences between the sites.

During the campaign three different pollution events were observed with increased pollutant concentrations. The increased concentration during these episodes were due to both trapping of local pollutants near the boundary layer and long-range and regional transport of pollutants to Helsinki metropolitan area. The local road vehicle emissions increased the particle number concentrations, especially sub-10 nm particles, and long-range and regional transported aged particles increased the PM mass and particle size.

https://doi.org/10.5194/egusphere-2024-2235
Preprint. Discussion started: 7 October 2024

1 Introduction

Exposure to increased particulate and gaseous pollutants can have adverse health effects on human health (Atkinson et al., 2014). Especially exposure to elevated concentrations of particulate matter is estimated to cause 3.3 million premature deaths/year on the global level (Lelieveld et al., 2015). Fine particles (D_p < 2.5 µm) are harmful since they can be transported deep into the human respiratory tract (Zanobetti et al., 2014). Especially ultrafine particles (D_p < 0.1 µm) may cause serious health problems since they can enter even deeper to the respiratory tract (Schraufnagel, 2020) and their concentration can be very high near local sources e.g. near heavily trafficked streets and highways or in street canyons (Pirjola et al., 2017; Trechera et al., 2023).

In earlier studies it has been shown that main local anthropogenic sources in Helsinki metropolitan area are direct vehicular emissions, road dust, and residential wood burning (Aurela et al., 2015; Carbone et al., 2014; Järvi et al., 2008; Saarikoski et al., 2008; Savadkoohi et al., 2023). Especially the concentration of ultrafine particles can increase near heavily polluted streets and street canyons during the morning and evening rush hours (Hietikko et al., 2018; Lintusaari et al., 2023; Okuljar et al., 2021; Trechera et al., 2023). In addition to local sources, long-range or regional transportation increases pollutant concentrations in Helsinki metropolitan area occasionally (Niemi et al., 2004, 2005, 2009). Local pollutants, mainly vehicle exhaust emissions, increase the particle number concentration due to the increased concentration of ultrafine particles (Rönkkö et al., 2017). In contrast long-range or regionally transported particles increase the concentration of particulate mass due to the larger size of the aged aerosol particles. Lung deposited surface area (LDSA) is used to predict the health effects related to particle deposition in the lung alveoli of particulate matter. Increased LDSA concentrations are connected to both increased number concentrations of ultrafine particles and increased particle size during episodes with long-range or regional transported aerosol (Kuula et al., 2020; Lepistö et al., 2023a; Liu et al., 2023).

In addition to temporal and diurnal variation of pollutant sources, local meteorology affects the pollutant concentrations in Helsinki metropolitan area. Especially wind speed may either decrease or increase pollutant concentrations. Concentrations of gaseous and particulate pollutants from nearby sources like motor vehicle exhausts decrease together with increasing wind speed due to more effective ventilation (Teinilä et al., 2019). On the other hand, concentration of coarse particles (D_p > 2.5 µm) may increase due to resuspension of street dust during windy periods. Volatile organic compounds emitted from motor vehicle engines can produce secondary organic aerosol (SOA, e.g., Gentner et al., 2017). Cold periods during wintertime cause stagnant conditions with low mixing height trapping the pollutants in the boundary layer and increasing their concentrations. Snow cover, rain, and wet snow inhibit the resuspension of street dust during wintertime.

A five-week intensive campaign at a Traffic Supersite was conducted during winter 2022 in Helsinki, Finland. The aim of the study was to investigate the role of wintertime conditions in aerosol formation and precursor gases, black carbon emissions, emission sources, and their influence on particles' physical and chemical properties. Dispersion of street canyon emissions were also studied using mobile measurements with the Aerosol and Trace-gas mobile laboratory by Tampere University (ATMo-Lab) near and at the measurement site. Particle physical and chemical properties were measured also at an urban background station (UB Supersite) during the campaign.

https://doi.org/10.5194/egusphere-2024-2235
Preprint. Discussion started: 7 October 2024

2 Experimental

2.1 Measurement sites

2.1.1 Traffic Supersite, Mäkelänkatu

The Traffic Supersite station was the principal measurement site during the winter campaign. The Traffic Supersite station is an urban measurement station operated by the Helsinki Region Environmental Services Authority (HSY), located in a street canyon on the street Mäkelänkatu (60.19654 N, 24.95172 E) in Helsinki (Fig. 1). At the Traffic Supersite, a continuous monitoring of urban air quality together with detailed measurements of particle physical and chemical properties is taking place. An additional measurement container was placed next to the Traffic Supersite station for installing additional measurement devices during the intensive campaign.

Mäkelänkatu street, next to the Traffic Supersite station, consists of six lanes, two rows of trees, two tram lines and two pavements, resulting in a total width of 42 m in the vicinity of the Traffic Supersite station. More detailed descriptions of the site and its air flow patterns are found in Hietikko et al., 2018, Kuuluvainen et al., 2018 and Olin et al., 2020 during the measurement campaign, the average number of vehicles driving along the street during workdays was 17 000 per day and the share of heavy-duty vehicles was 10 % (statistics from the City of Helsinki).

2.1.2 Urban background supersite, SMEAR III, Kumpula

The SMEAR III measurement station is an urban background supersite (UB Supersite) located in Kumpula campus area (Fig. 1, Järvi et al., 2009) There is one main road nearby, approx. 150 m from the station, with a daily traffic load of approx. 50 000 vehicles also containing a considerable number of heavy-duty vehicles. However, the UB Supersite is less affected by the local traffic compared to the Traffic Supersite because of the markedly longer distance to the main road. The site is also affected by local residential wood combustion emissions especially during the winter months. A more detailed description of the UB Supersite surroundings is given in (Järvi et al., 2009).

At the UB Supersite aerosol particle physical and chemical properties and trace gases are continuously measured. During the intensive campaign additional instrumentation was placed at the UB Supersite (see below). The measurements at the UB Supersite were used to get information on the aerosol and trace gas properties in urban background areas.

2.1.3 Rural site, Luukki

Luukki measurement station operated by the HSY is a Helsinki metropolitan area background station situated in clean background area (20 km from the Traffic Supersite) with no major local pollution sources nearby. The increased concentrations of $PM_{2.5}$ and BC due to long range or regional transport of particulate matter are typically observed at Luukki measurement station together with those inside the city centre area. The concentrations of $PM_{2.5}$ and BC at Luukki measurement station were measured using Fidas 200 (Palas GmbH) and Multi-Angle Absorption Photometer (MAAP, Thermo Electron Corporation) instruments.

2.2 Instrumentation

2.2.1 Stationary measurements at Traffic Supersite and UB Supersite

SP-AMS

https://doi.org/10.5194/egusphere-2024-2235
Preprint. Discussion started: 7 October 2024

The chemical composition of aerosol particles was studied with a Soot Particle Aerosol Mass Spectrometer (SP-AMS, Aerodyne Research Inc) described in Onasch et al., 2012 at the Traffic Supersite. Shortly, AMS consist of a particle sampling inlet, a particle-size chamber, and a particle composition detection system. After entering through critical orifice and aerodynamic lenses, particles are size-separated in a time-flight chamber and vaporized either on a tungsten plate (600 °C) or with an intracavity Nd-YAG-laser (1064 nm). The resulting species are ionized by electron impaction (70 eV) and detected with Time-of-Flight mass spectrometry (ToF). In addition to non-refractory species such like organic aerosol (OA), sulphate, nitrate, ammonium and chloride, SP-AMS also measures refractory black carbon (rBC) as well as other refractory particulate material (e.g., metals).

In this study, SP-AMS was operated with a 60 s time-resolution of which half was measured in mass spectrum mode (bulk mass concentrations) and half in Particle Time-of-Flight (PToF) mode (mass size distributions). The size range covered by the SP-AMS was approximately from ~50 nm to 1 µm (vacuum aerodynamic diameter) which was achieved with the aerodynamic lens system. Composition dependent collection efficiency was calculated based on Middlebrook et al., (2012). The effective nitrate response factor and relative ionization efficiency (RIE) of ammonium (RIE_{NH4}: 4), and sulphate (RIE_{SO4}: 0.9) were determined by calibrating the instrument by using dried size-selective ammonium nitrate and ammonium sulphate particles. The default RIE values for organic aerosol (1.4) and chloride (1.3) were used. SP-AMS data was analysed using a standard AMS data analysis software (SQUIRREL v. 1.63B and PIKA v. 1.23B) within Igor Pro 6 (Wavemetrics, Lake Oswego, OR) and for elemental analysis of organics an Improved-Ambient method was used (Canagaratna et al., 2015). The sources of organic aerosol (OA) were investigated by Positive Matrix Factorization (PMF) using the SoFi Pro software package (version 8.4.0, Canonaco et al., 2013), which employes a multilinear engine (ME-2) as a PMF solver (Paatero, 1999).

ACSM

Chemical composition of particulate matter (PM_1) was measured continuously using an Aerosol Chemical Speciation Monitor (ACSM, Aerodyne Research Inc., Ng et al., 2011) at the UB Supersite. The ACSM characterises non-refractory aerosol species (total organics, sulphate, nitrate, ammonium, and chloride) with a time resolution of approximately 30 min. The ACSM measures particles that pass through the aerodynamic lens (50 % transmission range of the lens is 75−650 nm, Liu et al., 2007). The flow into the ACSM (controlled by critical orifice) was roughly 0.1 l min^{-1}, but in addition bypass flow of 3 l min^{-1} was used to get particles efficiently close to the inlet of ACSM. A cyclone (URG, URG-2000-30ED) was used before ACSM to remove particles larger than 2.5 µm (aerodynamic diameter) for preventing clocking the critical orifice.

GC−MS/FID

Volatile organic compounds (VOCs) and intermediate volatile organic compounds (IVOCs) containing 6 to 15 carbon atoms were measured with 1-hour time resolution using an in situ thermal desorption-gas chromatograph-mass spectrometer (TD-GC-MS) at the Traffic Supersite. Quantified compounds included 10 terpenoids, 15 alkanes, 20 aromatic hydrocarbons, 4 oxygenated aromatic hydrocarbons, and 8 polycyclic aromatic hydrocarbons (PAHs) (Table S1). The system consisted of TurboMatrix 350 connected to an online sampling accessory (TD), Clarus 680 (GC), and Clarus SQ 8 T (MS) all manufactured by PerkinElmer. GC column used was an Elite-5MS 60 m x 0.25 mm (i.d.), film thickness 0.25 µm (PerkinElmer). Sample was collected to the TD's Tenax-TA & Carbopack B dual absorbent cold trap

https://doi.org/10.5194/egusphere-2024-2235
Preprint. Discussion started: 7 October 2024

which was kept at 20 °C. Sampling was done approx. 3 m from street level above the container at Traffic Supersite. The inlet was 1/8-inch FEP line, and the outside portion was heated to be around 30 °C. Ozone was removed from the sample flow by guiding the flow through a 1/8-inch stainless steel tube heated to 120 °C. A flow of 300–800 ml min^{-1} was kept through the inlet from which the TD collected 30–45 min samples with a flow of 40 ml min^{-1}. More in depth description of the system and method can be found in (Helin et al., 2021).

Additional sorbent tube samples were collected at the UB Supersite. Samples were collected to Tenax-TA & Carbopack B dual absorbent tubes via modified sequential tube sampler (STS 25 Unit, PerkinElmer). Main modifications being an upgrade to the sampling pump and rain cover exchange to PFA from stainless steel. The STS unit consist of a carrousel that rotates on a timer placing the tubes to the slot for active sampling. The carrousel holds 24 tubes at a time and sampling time was set for 4 h making sampling sets approx. 4 days long. Sampling flow was kept around 100 ml min^{-1}. Tubes were then analysed in the laboratory with a similar TD-GC-MS setup as described above for in situ samples.

Non-methane hydrocarbons (NMHCs) containing 2–5 carbon atoms were sampled at the Traffic Supersite with collection to stainless steel vacuum canisters. The flow from ambient to the vacuum of the canisters were restricted by a critical orifice making sampling time 24 h. The canister walls were coated with silcosteel. Before analysis canisters were over pressurized with pure nitrogen (99.9999 %). From the pressurised canisters samples were collected to the cold trap of the Markes international Unity 2 via AirServer addon. The system had a Dean switch with dual column and detector setup. First column was DB-5MS 60 m x 0.25 mm (i.d.), film thickness 1 µm (Agilent) and after that the most volatile compounds (C2–C5) were directed to a second column CP-Al2O3/KCl 50 m x 0.32 mm (i.d.), film thickness 5 µm (Agilent) via the Dean switch. C2–C5 compounds were analysed with a flame ionization detector (FID) and rest with the MS. The setups GC/FID was Agilent 7890A and the MS Agilent 5975C.

NAIS

Two Neutral Cluster and Air Ion Spectrometers (NAIS, Airel Ltd, Manninen et al., 2016; Mirme and Mirme, 2013) were used to measure size and mobility distributions of aerosol particles and air ions at the Traffic Supersite station (NAIS 5-27) and at the UB Supersite station (NAIS12). Air ions of both polarities in the electric mobility range from 3.2 to 0.0013 $cm^2\ V^{-1}\ s^{-1}$ (~0.8–40 nm in mobility diameter) and the distribution of aerosol particles in the size range from ~2 nm to 40 nm were measured with a maximum time resolution of 1 s. Both instruments sampled via horizontal copper inlets with the sample flow rate of ~54 l min^{-1}.

CPCs

Two condensation particle counters (CPC), TSI model 3756 (UB Supersite) and Airmodus model A20 (Traffic Supersite) were used to measure particle number concentration time series. The TSI 3756 has a particle concentration range up to 300,000 cm^{-3} and size range down to 7 nm (Dp_{50}), and the maximum detectable particle size > 3 µm. Inlet flow rate of 1.5 l min^{-1} was used. The Airmodus A20 was used with a bifurcated flow diluter (dilution ratio 8.5), which expands concentration range up to 250,000 cm^{-3} in single particle counting mode. The particle size range measured was from 5.4 nm (Dp_{50}) to 2.5 µm. In both CPC types, butanol (n-Butyl alcohol) was used as a working fluid and data was collected at 1 min time resolution.

https://doi.org/10.5194/egusphere-2024-2235
Preprint. Discussion started: 7 October 2024

nCNC with AND

An Airmodus Nanoparticle Diluter (AND) (Airmodus Ltd, Lampimäki et al., 2023) was used to dilute sample air upstream of a nano-Condensation Nucleus Counter (nCNC) system (Airmodus Ltd, Vanhanen et al., 2017) at the Traffic Supersite. The nCNC measures the particle activation size distribution between ca. 1 and 4 nm by scanning the cut-off size. The default dilution factor of 5 was used by using dry compressed air in the dilution, which also allowed drying of the sample to < 30 % relative humidity (RH). In the preset study the Ion Precipitator (IOP) voltage (1 kV) of AND was sequentially switched on and off with a custom-made MATLAB based program. IOP can be used to scavenge ions at the mobility diameters below ~8 nm, while the larger (> 10 nm) particles are passing through the IOP with the 50 % cut-off size around 9 nm. Thus, the IOP mode could provide additional information on the charged fraction of recently formed particles or clusters.

MAAP

Black carbon concentration was measured using a Multi-Angle Absorption Photometer (MAAP, Thermo Electron Corporation, Model 5012, Petzold and Schönlinner, 2004) at the Traffic Supersite and at the UB supersite stations. The MAAP determines the absorption coefficient (σAP) of the particles deposited on a filter by a simultaneous measurement of transmitted and backscattered light. The σAP is converted to BC mass concentrations by the instrument firmware using a mass absorption cross section of 6.6 $m^2\ g^{-1}$, Petzold and Schönlinner, 2004. The flow rate of the MAAP at the Traffic Supersite was 11 l min^{-1} and 5 l min^{-1} at the UB Supersite. Both MAAP instruments measured with one minute time resolution and Cyclone/PM_1 inlet was used to cut-off particles above 1 µm.

AE33

An AE33 dual spot aethalometer (Magee Scientific, Slovenia) was used to measure the aerosol light absorption and corresponding carbon mass concentrations at seven different wavelengths between 370 and 950 nm (Drinovec et al., 2015; Hansen et al., 1984) at the Traffic Supersite and at the UB Supersite. The flow rate of the AE33 was 5 l min^{-1} and the used filter tape was PTFE-coated glass fibre filter (no. M8060) at both stations. The cut-off size of the sample was 1 µm at both station and it was achieved using a sharp cut cyclone (Model SCC1.197, BGI Inc., Butler, NJ, USA).

AQ Urban

The alveolar LDSA concentration of aerosol particles between 10 and 400 nm were measured with the Pegasor AQ™ Urban instrument (Pegasor Ltd., Finland) at the Traffic Supersite and at the UB Supersite (Kuula et al., 2020).

DMPS

A Differential Mobility Particle Sizer (DMPS) was used to measure particle size distributions from 11 to 800 nm (Traffic Supersite) and from 3 to 800 nm (UB Supersite) using a Vienna type Differential Mobility Analysers and an Airmodus A20 model CPC (Traffic Supersite) and TSI 3025 CPC (UB Supersite).

Picarro

Gas analyser for carbon monoxide (CO), carbon dioxide (CO_2) and methane (CH_4) at both sites was a Picarro G2401 manufactured by Picarro Inc. (Santa Clara, CA). It also measures water vapor concentration, based on which it calculates

https://doi.org/10.5194/egusphere-2024-2235
Preprint. Discussion started: 7 October 2024

dry concentrations for other components. The instrument is based on cavity ringdown spectroscopy (CRDS), in which long optical path length allows measurements with high precision and stability using near-infra-red laser sources.

The Kumpula instrument close to the UB Supersite took its sample air from the roof of the five-store Finnish Meteorological Institute's building ca. 30 m above the ground. The sample air was dried with a Nafion dryer run in reflux mode. The supersite Picarro was run with non-dried sample air. Both instruments were calibrated with WMO/CCL (World Meteorological Organization/Central Calibration Laboratory) traceable gases.

Filter sampling and chemical analysis

In addition to online measurements, daily PM_{10} PAH filter samples and one or two PM_1 filter samples per day for sugar anhydride (levoglucosan, mannosan and galactosan) and EC/OC analyses were collected at the Traffic Supersite. Quartz fibre filters (PALL, Tissuquartz 2500-QAT-UP, NY, USA) were used as sampling substrates for PM_1 samplings and the used flow rates were 20 l min^{-1} for sugar anhydride and EC/OC samplings.

Other instrumentation

Concentration of particulate mass ($PM_{2.5}$ and PM_{10}) were measured with Fidas 200 (Palas) instrument at the Traffic Supersite. Concentrations of gaseous compounds were also continuously measured at the Traffic Supersite. APNA 370 (Horiba) instrument was used for measuring the concentrations of NO_x (APNA 370) and O_3 (APOA 370), APMA 360 (Horiba) was used to measure the concentration of CO and LI-7000 (LICOR) was used to measure the concentration of CO_2. Particle scattering coefficient was measured with a nephelometer (TSI, model 3610) at the Traffic Supersite. The measurement devices at the UB Supersite are shown in Table S2.

Back trajectories of air masses arriving to the measurement site were calculated using the NOOA HYSPLIT model (Rolph et al., 2017; Stein et al., 2015). The 96-hour back trajectories were calculated for every hour for 200 m above sea level. Mixing height was calculated using model developed at Finnish Meteorological Institute (MPP-FMI, Karppinen et al., 2000) The data analysis was made using the R software (R Core Team 2022) and R package openair (Carslaw and Ropkins, 2012). Hourly mean concentrations of the measured components were used in the following discussion unless otherwise mentioned. The used timestamp for hourly mean concentrations is the end hour and the used datetime is local time.

PAH analyses

The concentrations of 6 PAHs (benzo(a)anthracene, benzo(b)fluoranthene, benzo(k)fluoranthene, benzo(a)pyrene, indeno(1,2,3-cd) pyrene, dibenz(a,h)anthracene) were analysed from daily PM_{10} samples using a gas chromatograph-mass spectrometer (GC-MSMS, Agilepicant 7890A and 7010 GC/MS Triple Quadrupole). For the analysis, the samples were ultrasonic extracted with toluene, dried with sodium sulphate, and concentrated to 1 ml. For chromatographic separation, the HP-5MS UI column (30 m x 0.25 mm i.d., film thickness 0.25 µm) and 2 m pre-column (same phase as analytical column) were used. Helium (99.9996%) was used as a carrier gas with a flow of 1 ml min^{-1}. The temperature program started at 60 °C with a 1 min hold, followed by an increase of 40 °C min^{-1} 1 to 170 °C, and 10 °C min^{-1} to 310 °C with a hold of 3 min. Deuterated PAH compounds (Naphthalene-d8, Acenaphthene-d10, Phenanthrene-d10, Chrysene-d12, Perylene-d12, PAH-Mix 31D, Dr. Ehrenstorfer) were used as internal standards and were added to an extraction solvent

https://doi.org/10.5194/egusphere-2024-2235
Preprint. Discussion started: 7 October 2024

before extraction. External standards (PAH Mix-137, Polynuclear aromatic hydrocarbons Mix, Dr. Ehrenstorfer) with five different concentration levels were used. In the analysis of benzo(a)pyrene, EN 15549 (2008) standard was followed. Measurement uncertainty was calculated from the validation data (Guide Nordtestin TR537) for the target value (0.1 ng m^{-3}) that value was found to be 25 %. The analysis method is accredited (SFS-EN ISO/IEC 17025:2017). The method has been previously described in detail by Vestenius et al., 2011.

Sugar anhydride analyses

The concentration of monosaccharide anhydrides (levoglucosan, mannosan and galactosan) were analysed from the PM_1 samples using a high-performance anion-exchange chromatography-mass spectrometry (HPAEC-MS). The HPAEC-MS system consists of a Dionex ICS-3000 ion chromatograph coupled with a quadrupole mass spectrometer (Dionex MSQ). The HPAEC-MS system had 2 mm CarboPac PA10 guard and analytical columns (Dionex) and potassium hydroxide (KOH) eluent. The used ionization technique was electrospray ionization. The analytical method is similar than described in Saarnio et al., 2010, except that the used internal standard was methyl-β-D-arabinopyranoside. A 1 cm^2 punch of the quartz fibre filter was extracted into 5 ml of MQ water with internal standard concentration of 100 ng ml^{-1} and the HPAEC-MS was utilized for determination of MA: s at m/z 161. The uncertainty of the analyses was typically 10–15 % and even larger (25 %) when the analysed concentration was low.

Other measurements during the campaign

At the Traffic Supersite gaseous sulfuric acid (H_2SO_4) was sampled and measured in the same way as described in Olin et al., 2020 with a nitrate-ion based chemical-ionization atmospheric-pressure-interface time-of-flight mass spectrometer (nitrate CI-API-TOF-MS, Aerodyne Research Inc. USA and Tofwerk AG Switzerland).

Enhanced Trace Level SO_2 Analyser (Thermo Scientific™, Model 43i-TLE) was employed at the measurement container next to the Traffic Supersite in between January 29 and February 22. Data was collected in 20 s time resolution with the instrument frow rate of 0.5 l min^{-1}.

The concentrations of particulate OC and EC were analysed using a thermal-optical OCEC aerosol analyser (model 5L, Sunset Laboratory Inc., Tigard, OR, US, (Birch and Cary, 1996)). In this study EUSAAR-2 protocol was used (Cavalli et al., 2010).

Results of these other measurements are not presented in this paper.

2.2.2 ATMo-Lab measurements

In addition to the stationary measurement stations, the Aerosol and Trace-gas mobile laboratory by Tampere University (ATMo-Lab) was utilized in both stationary and mobile measurements between 18 January and 16 February 2022. Stationary measurements were conducted on the kerbside, next to the Traffic Supersite and along a side street (Anjalantie, 60.197725 N, 24.957364 E) nearby. Mobile measurements included a park and a street canyon section of the main street (Mäkelänkatu) along which the measurement stations were located and its side streets with apartment buildings. Stationary measurement locations along with the driving route are presented in Fig. 1. Measurements were conducted daytime between 6:30 and 19:30 as is shown in Fig. S1.

https://doi.org/10.5194/egusphere-2024-2235
Preprint. Discussion started: 7 October 2024

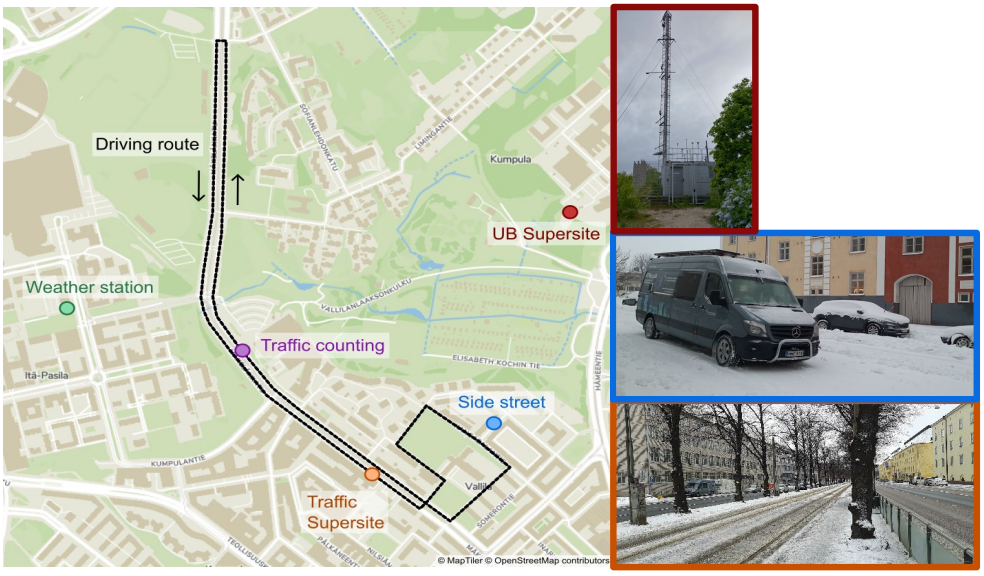

Figure 1. Stationary measurement locations and the driving route of the Aerosol and Trace-gas mobile laboratory.

The sample air was taken from an inlet located above the ATMo-Lab's windscreen and distributed to the instruments at the back of the van. The risk of self-sampling during driving measurements was minimal as the exhaust pipe is at the rear end of the van. The van itself is Euro VI compliant. Measurement setup inside the ATMo-Lab is shown in Fig. S1. Key measurement target of the ATMo-Lab measurements was ultrafine particles. Particle number concentrations were measured using a Condensation Particle Counter Battery (CPCB) and an Electrical Low-Pressure Impactor (ELPI+, Dekati Ltd). The CPCB consisted of a combination of a Particle Size Magnifier (PSM) and a Condensation Particle Counter (CPC) in parallel with four CPCs with different cut-off sizes. Working principle of PSM is described in (Vanhanen et al., 2011). Exact CPCB instruments were A11 nCNC (combination of PSM and CPC, Airmodus Ltd), CPC 3756 (TSI Inc), CPC 3775 (TSI Inc), CPC A20 (Airmodus Ltd), and CPC A23 (Airmodus Ltd). Respectively, total particle number concentrations were simultaneously measured for size ranges > 1.3 nm, > 2.5 nm, > 4 nm, > 10 nm, and > 23 nm with a time resolution of one second. Sample air was diluted before entering to the CPCB using a bifurcated flow diluter, including a static mixer, with dilution ratio of 17.

At the same time, ELPI+ measured the particle number size distribution with its 14 impactor stages in a size range from 6 nm to 10 µm. The operation principle of ELPI is described in (Keskinen et al., 1992) and (Marjamäki et al., 2000), and the calibration of renewed ELPI+ is presented in Järvinen et al., 2014. ELPI+ was also used to measure particle lung deposited surface area (LDSA) and mass (PM). The stage-specific conversion from electric current data of ELPI+ to LDSA concentration enable measurement of the LDSA concentration and size distribution with the whole ELPI+ size range (Lepistö et al., 2020). LDSA was also measured by a sensor type device Partector (Naneos particle solutions GmbH). Furthermore, $PM_{2.5}$ concentrations were calculated by integrating over the particle number size distribution measured with ELPI+ assuming spherical particles with unit density. Similar assumptions were made with particle number and LDSA size distributions.

https://doi.org/10.5194/egusphere-2024-2235
Preprint. Discussion started: 7 October 2024

Non-volatile particle number was measured with two prototype instruments originally developed for renewed demands of vehicle inspection: a Mobile Particle Emission Counter (MPEC+, Dekati Ltd) and a Pegasor sensor (Pegasor Ltd). Latter sampled first from the roof of the ATMo-Lab (18 January to 2 February) after which it was also connected to the main line (2 February to 16 February). A combination of a thermodenuder followed by a CPC was used as a reference for the prototype instruments. The thermodenuder model was the same as in Heikkilä et al., 2009 and (Amanatidis et al., 2018). The CPC used was a model CPC 3775 (by TSI Inc) with altered cut-off diameter (4 nm, 10 nm, or 23 nm) as the cut-off size was changed twice during the measurements. The cut-off size was changed by altering the condenser temperature of CPC according to a laboratory calibration.

For the analysis of particles' chemical composition and especially black carbon, the ATMo-Lab setup included a SP-AMS and an AE33 aethalometer like the instruments described in the stationary measurements section. For the driving measurements SP-AMS menu was switched from the 60 s time-resolution (30 s mass spectrum mode + 30 s PToF-mode) to a 24 s time-resolution operation mode in which 14 s was measured in a mass spectrum mode and 10 s in a PToF-mode. From the gaseous compounds, the ATMo-Lab was equipped to measure CO_2 (LI-7000, LI-COR Corp) and NO (Model T201, Teledyne Technologies Inc).

In stationary measurement locations, particles were collected with and without thermal treatment on holey-carbon grids by a flow-through sampler. This was done for elemental composition and morphology study with (Scanning) Transmission Electron Microscope (S/TEM) accompanied by energy-dispersive spectrometry (EDS).

3 Results

3.1 General description of the measurement campaign.

3.1.1 Meteorology

The intensive campaign took place between 17 January and 22 February 2022, which is typically the coldest winter period with a minimum amount of sunlight. Temperature, relative humidity, wind speed and wind direction during the winter campaign measured at roof level in Pasila (53 m, Fig. 1) about 1 km from the Traffic Supersite are shown in Fig. 2. Mean temperature during the measurement campaign was -1.4 °C (range −10.0–2.9 °C) and mean relative humidity was 89 % (range 58–100 %). The temperature was most of the time near 0 °C. The prevailing wind direction during the measurements were from south to south-east and the mean wind speed was 4.9 m s^{-1} (range 0.59–11.4 m s^{-1}). The average mixing height was 408 m (range 58–844),

Surface inversion episodes take place during the coldest winter days with low temperature and wind speed causing gaseous and particulate pollutants to be accumulated in the boundary layer (Barreira et al., 2021; Teinilä et al., 2019). Two cold periods together with low wind speed and low mixing height took place during the campaign (Fig. 2) enabling surface inversion episodes. In general, local traffic is an important source of gaseous and particulate pollutants at the Traffic Supersite. The air quality in Helsinki is also affected by long-range transported pollution episodes (Niemi et al., 2004, 2005, 2009; Leino et al., 2014; Pirjola et al., 2017) Local wood burning due to heating of detached houses in winter increase air pollutant concentrations in Helsinki. Majority of this wood burning is taking place outside city centre in residential suburban area (Kangas et al., 2024). During wintertime the long-range and regional transported air masses consist more particulate pollutants connected to biomass burning (Pirjola et al., 2017; Teinilä et al., 2022).

https://doi.org/10.5194/egusphere-2024-2235
Preprint. Discussion started: 7 October 2024

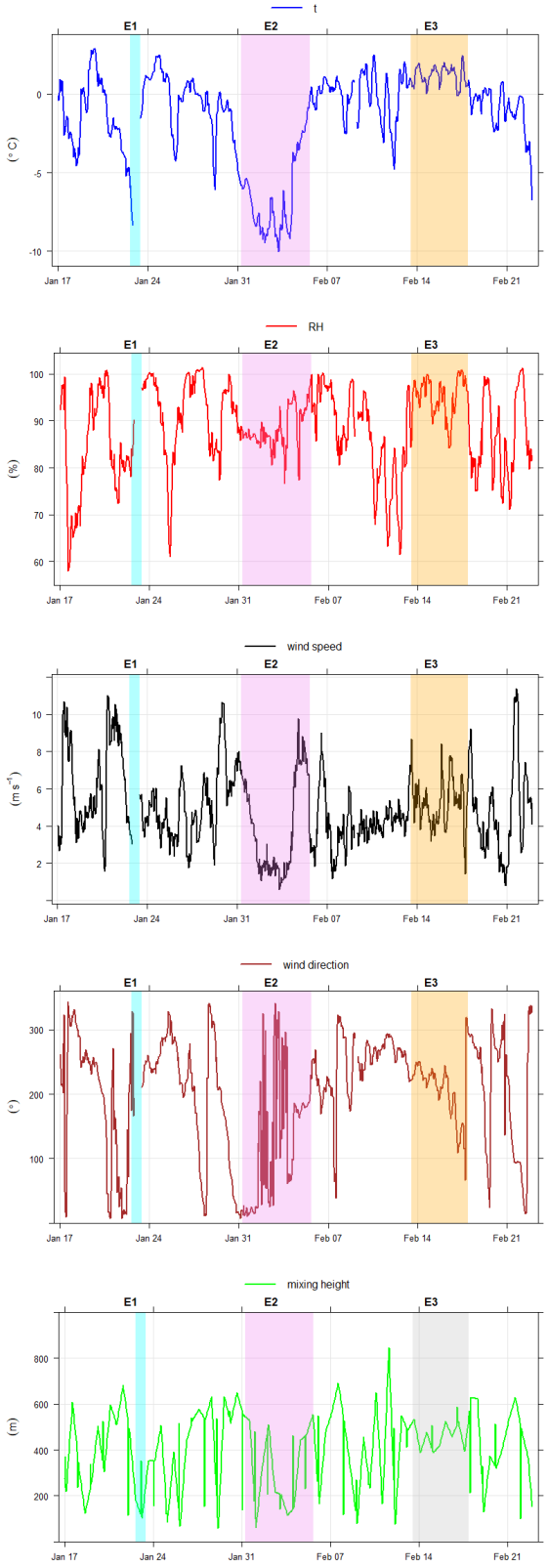

https://doi.org/10.5194/egusphere-2024-2235
Preprint. Discussion started: 7 October 2024

Figure 2. Temperature, relative humidity, winds speed, wind direction and mixing height during the measurement period measured at Pasila. The three episodes are coloured in the figure.

3.1.2 Traffic frequencies

Traffic frequencies near the Traffic Supersite station are shown in Fig. 3. The exact location for traffic counting is presented in Fig. 1. Traffic frequency towards the city centre (south) starts to increase around 6:00 and reach its maximum between 9:00 and 10:00. The afternoon traffic frequency peak between 17:00 and 18:00 is slightly lower compared to the morning. Traffic frequencies away from the city centre (north) behave opposite trend showing maximum frequencies during afternoon hours. The maximum frequencies out of the city centre are achieved at the same time than those towards to city centre. There are no rush hours during the weekends (Fig. 3) and traffic frequencies starts to slowly increase before noon and show their maximum between 18 and 19 towards both directions. The measurement site is located near to the lines leading towards the city centre (south).

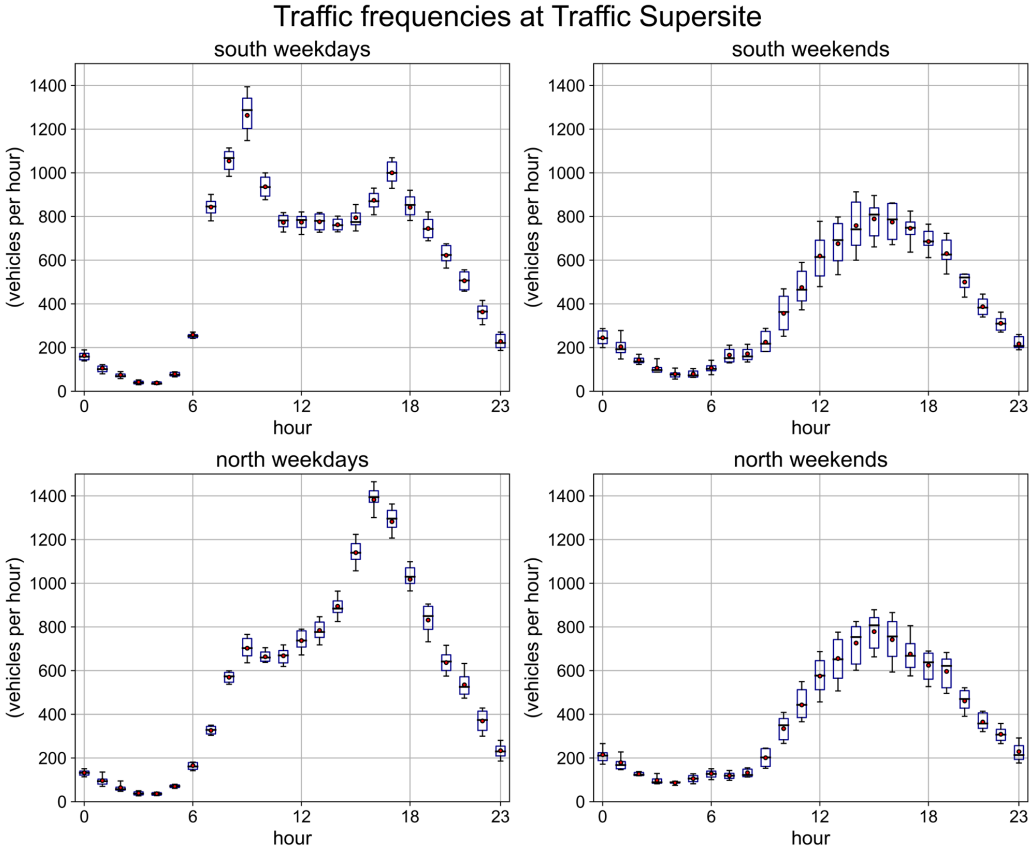

Figure 3. Hourly traffic frequencies to south (towards city centre) and to north during workdays and weekends near the Traffic Supersite. The Traffic Supersite station is placed on a pavement on the south traffic side in Mäkelänkatu.

https://doi.org/10.5194/egusphere-2024-2235
Preprint. Discussion started: 7 October 2024

3.1.3 Particle chemical and physical properties during the campaign

The mean concentrations of $PM_{2.5}$ and $PM_{2.5–10}$ were 5.2 and 3.3 µg m^{-3}, respectively, during the whole campaign. The five year average $PM_{2.5}$ concentration between 2015 and 2019 at the Traffic Supersite was 7.2 µg m^{-3} (Barreira et al., 2021). The $PM_{2.5–10}$ concentration was relatively low during the campaign. This is due to rainfall, snowfall, and snow covering the streets during the campaign which inhibited the formation and re-suspension of street dust. Most of the street dust is in coarse particle size, but it is in some degree also in fine particle size range. The lack of street dust episodes in winter explains, at least partly, why the mean $PM_{2.5}$ is also lower than that measured at the Traffic Supersite throughout in years 2015–2019 (Rönkkö et al., 2023b). Some pollution episodes can be observed, and they will be analysed in section 3.1.5.

The mean concentrations of BC, NO, and NO_2 were 0.61 µg m^{-3}, 13.7 µg m^{-3}, and 22.2 µg m^{-3}, respectively, at the Traffic Supersite. The mean particle number (PN) concentration at the Traffic Supersite during the measurement period was 18 473 p cm^{-3} but mean hourly concentrations of PN higher than 80 000 p cm^{-3} were also measured (Fig. S3). The PN concentration of particles larger than 2.5 nm in the ATMo-Lab measurements (Dp_{50}: 2.5 nm) next to the Traffic Supersite was considerably higher than the one measured at the Supersite (Dp_{50}: 5.4 nm) (Fig. S4), showing the effect of road traffic in the emissions of the smallest nanoparticles (e.g. Hietikko et al., 2018; Lintusaari et al., 2023; Rönkkö et al., 2017). In general, it should be noted that the measured PN concentrations may differ notable depending on the used instrument cut-off size as also seen when comparing ATMo-Lab measurements with cut-off sizes 2.5 nm and 10 nm (Fig. S5, Rönkkö et al., 2023a). The mean hourly LDSA concentration at the Traffic Supersite was 13.6 $\mu m^2\ cm^{-3}$ during the measurement period (Fig. S2) and the highest hourly mean LDSA concentration during the measurement period was 62 $\mu m^2\ cm^{-3}$.

Mean concentrations of organics, sulphate, nitrate, ammonium, and chloride measured with the SP-AMS (PM_1) were 2.0 µg m^{-3}, 0.6 µg m^{-3}, 0.6 µg m^{-3}, 0.4 µg m^{-3}, and 0.07 µg m^{-3}, respectively. The sum of the concentrations of the measured chemical components (organic and inorganic species from SP-AMS and BC from MAAP) showed a high correlation coefficient (square of Pearson correlation, R^2) against $PM_{2.5}$ (0.92).

3.1.4 Volatile organic compounds

The mean concentrations of the continuously measured C6–C15 aromatic hydrocarbons, alkanes, PAHs and terpenoids were 2.2, 0.94, 0.037 and 0.16 µg m^{-3}, respectively at the Traffic Supersite. Offline samples of C2–C5 NMHCs collected during the shorter periods showed that light alkanes were the most significant compound group detected (Fig. 4). However, larger, and more reactive compounds with higher SOA formation potentials are expected to have stronger impacts on the local chemistry even with lower concentration. Compounds with 6 to 9 carbon atoms were mostly aromatic hydrocarbons and for higher carbon masses (C10–C11) alkanes and terpenes had major contribution (Fig. 4). Contribution of PAHs was very low. Major contribution of aromatic hydrocarbons was expected due to traffic as a major local source of VOCs. Higher alkanes (C10–C15), which had highest contribution for IVOCs (Fig 6. C10–C15), are commonly found especially in diesel emissions (Marques et al., 2022; Wu et al., 2020). Also, terpenoids, which are traditionally considered as biogenic compounds, had relatively high concentrations during this winter period. Emissions from the vegetation are expected to be negligible due to cold weather and this indicates anthropogenic sources for these compounds. They are commonly found for example in personal care and cleaning products (Coggon et al., 2021; Steinemann, 2015). In earlier studies terpenoids have been detected also during wintertime in the urban background air in Helsinki (Hellén et al., 2012).

https://doi.org/10.5194/egusphere-2024-2235
Preprint. Discussion started: 7 October 2024

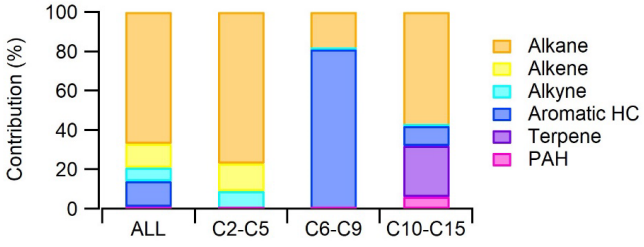

Figure 4. Contribution of different compounds groups on measured concentrations during the periods when all VOCs with 2 to 15 carbons (ALL) were measured. C2–C5 = VOCs with 2 to 5 carbons, C6–C9=VOCs with 6 to 9 carbon atoms, and C10–C15=VOCs/IVOCs with 10 to 15 carbon atoms at the Traffic Supersite.

3.1.5 Pollution episodes

During the campaign three episodes with enhanced particulate and gaseous pollutant concentrations were observed. The duration of these episodes is shown in Table 1. The names from E1 to E3 will be used for these episodes in the proceeding chapters.

The timeseries in Fig. 5 show the concentrations of fine ($PM_{2.5}$) and coarse ($PM_{2.5–10}$) particles at the Traffic Supersite, UB Supersite, and Rural site. $PM_{2.5}$ showed elevated concentrations during the three episodes at the Traffic Supersite. $PM_{2.5–10}$ concentration did not show long lasting increase in its concentration during these episodes, but shorter high peaks were observed. The increased concentrations of $PM_{2.5}$ is due to both, of trapping of local pollutants on boundary layer during cold periods and the effect of long-range or regional transport of pollutants at the Traffic Supersite station. The increased $PM_{2.5}$ concentration at all sites, also including the Rural site, indicate that long-range or regional transport had an important effect on the air quality in Helsinki Metropolitan area during these episodes. The concentration of $PM_{2.5–10,}$ on the other hand, was affected by wind speed and local snow cover or by wet street surface when the temperature was near or above 0 °C (during E3). Also, coarse particles are not typically transported from very long distances. The source of the short-lasting peaks in $PM_{2.5–10}$ concentration may be due to some local activity near the stations (Traffic Supersite and UB Supersite. together with favourable meteorological conditions as well as non-exhaust emissions from traffic.

https://doi.org/10.5194/egusphere-2024-2235
Preprint. Discussion started: 7 October 2024

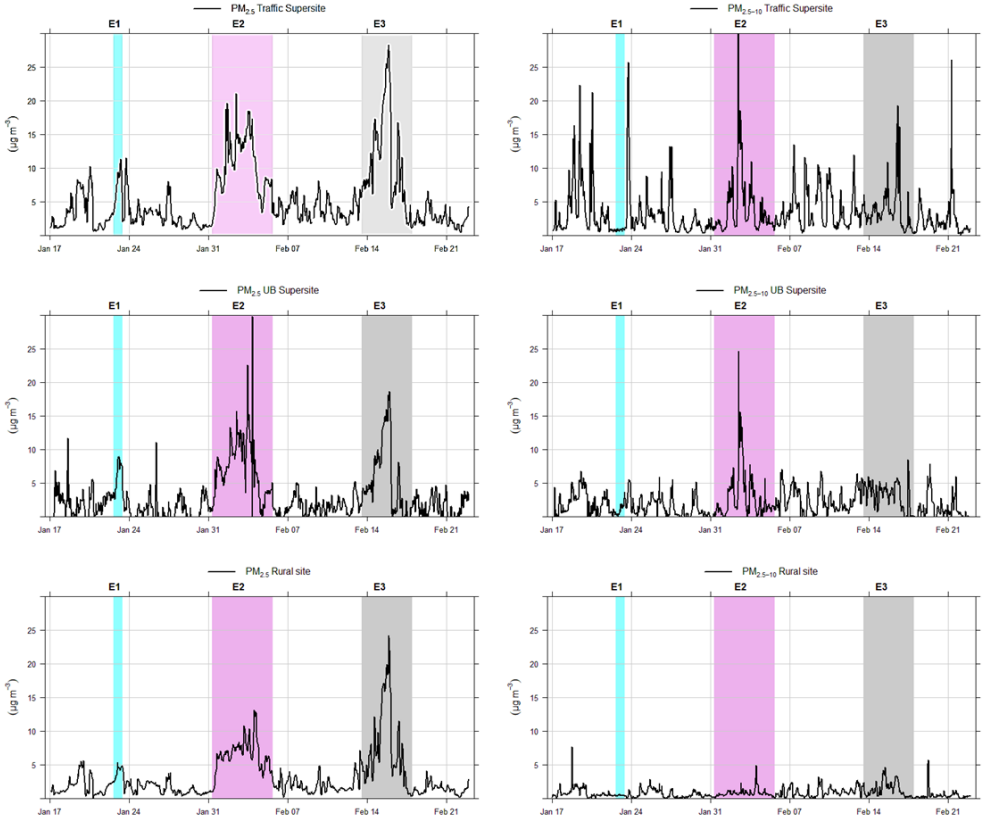

Figure 5. Concentrations of $PM_{2.5}$ and $PM_{2.5\text{-}10}$ at the Traffic Supersite, UB Supersite and Rural site. The three episodes are colored in the figure.

Table 1. Traffic frequencies and average concentrations of measured components during the traffic (averages without episodes) dominated period on workdays and weekends and their averages during three different episodes at the Traffic Supersite.

Compound	**Traffic workdays**	**Traffic weekends**	**E1** 22.1.2022 15:00 – 23.1.2022 10:00	**E2** 31.1.2022 07:00 – 5.2.2022 16:00	**E3** 13.2.2022 12:00 – 17.2.2022 23:00
Traffic frequencies *(vehicles per hour)*	1109	767	738	1126	1201
PN$_{>5nm}$ *(p cm^{-3})*	19901	11976	17751	23650	17143
LDSA *(μm^2 cm^{-3})*	12.0	8.0	16.1	22.2	16.9
PM$_{2.5}$ *(μg m^{-3})*	3.2	3.1	7.1	10.3	11.0
PM$_{2.5\text{-}10}$ *(μg m^{-3})*	3.7	2.6	0.8	4.1	3.8
NO *(μg m^{-3})*	13.7	4.9	4.5	26.4	11.7

https://doi.org/10.5194/egusphere-2024-2235
Preprint. Discussion started: 7 October 2024

NO_2 *(μg m^{-3})*	23.1	13.2	21.6	28.0	23.3
BC *(μg m^{-3})*	0.46	0.29	0.96	1.18	0.90
CO *(ppb)*	164	164	202	253	210
CO_2 *(ppm)*	435	432	438	450	440
CH_4 *(ppb)*	2015	2021	2048	2076	2056
O_3 *(μg m^{-3})*	46	55	34	25	42
Toluene *(μg m^{-3})*	0.62	0.60	0.85	0.78	0.60
α-pinene *(μg m^{-3})*	0.033	0.029	0.086	0.068	0.040
Particulate organics *(μg m^{-3})*	1.12	0.94	3.07	4.54	4.25
Sulphate *(μg m^{-3})*	0.20	0.24	1.56	2.12	0.84
Nitrate *(μg m^{-3})*	0.26	0.19	1.78	1.58	1.48
Ammonium *(μg m^{-3})*	0.16	0.13	1.04	1.07	0.78
Chloride *(μg m^{-3})*	0.05	0.04	0.08	0.06	0.18
HOA *(μg m^{-3})*	0.17	0.09	0.14	0.49	0.18
BBOA *(μg m^{-3})*	0.08	0.08	0.10	0.14	0.16
SV-OOA *(μg m^{-3})*	0.15	0.11	0.28	0.49	0.17
LV-OOA *(μg m^{-3})*	0.27	0.25	0.14	0.33	0.66
LV-OOA (BB) *(μg m^{-3})*	0.11	0.16	1.12	1.64	1.71
Tr-OOA *(μg m^{-3})*	0.23	0.15	0.34	0.36	0.17

The highest increase in their concentrations during the episodes at Traffic Supersite were found for secondary inorganics (sulphate, nitrate, and ammonium), total organics, measured with SP-AMS and BC measured in PM_1 (Table 1). α-pinene, known as a SOA precursor, had also clearly higher concentrations during the periods E1–E3. Concentration of chloride showed a clear increase only during period E3. Similar increase in the concentrations of BC (Fig. 6) and measured inorganics and total organic matter was seen also at the UB Supersite (Fig. S6). The increased $PM_{2.5}$ concentration is thus connected of formation of secondary particulate matter together with increased concentration of total organic matter.

Particle number concentrations showed slight increase during the E2 episode at both sites and in ATMo-Lab with cold temperatures (Table 1 and Table S3, Fig. S3) which indicates that, in addition to long-range transported pollutants, local traffic emissions were also trapped on the boundary and layer affected the air quality at the measurement site. Also, higher concentrations of α-pinene with short atmospheric lifetime (~few hours) indicated local influence. Episode E1 took place during the weekend so its concentrations should be compared against the traffic weekend situation.

https://doi.org/10.5194/egusphere-2024-2235
Preprint. Discussion started: 7 October 2024

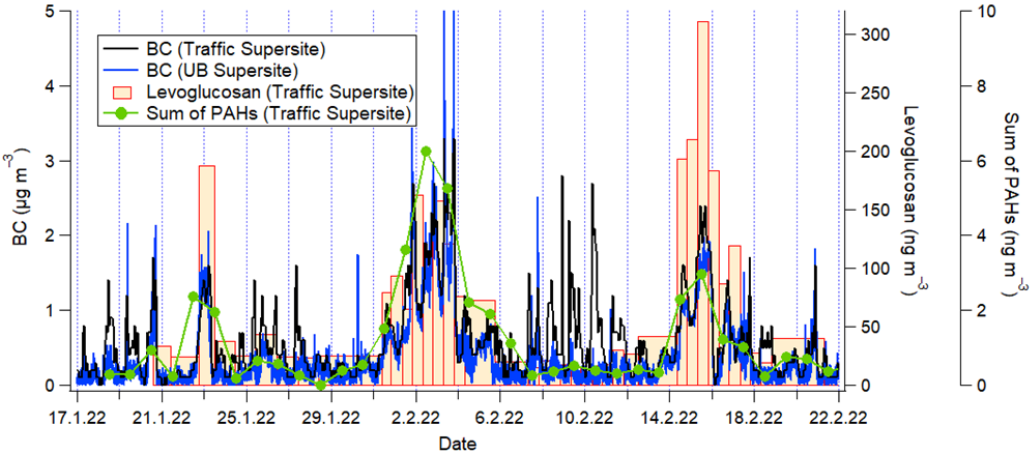

Figure 6. Concentrations of BC at the Traffic Supersite and at the UB Supersite as well as the concentrations of levoglucosan and the sum of measured PAH compounds at the Traffic Supersite, analysed from filter samples. The filter sample times are the mean of sampling start and stop times. The PAH sampling time during 15 February consisted only 12 hours.

Concentrations of major gaseous and chemical components were measured also at the UB Supersite during the campaign (Table S3). The concentrations of traffic related components PN, LDSA and NO_2 were on average 2–3 times higher at the Traffic Supersite compared to the UB Supersite during non-episodic workdays which is expected due to the much less influence of traffic at the UB Supersite. The same was also for $PM_{2.5}$ concentrations between the two sites indicating its local source at the Traffic Supersite. Concentrations of these compounds were similar or only slightly lower during non-episodic weekends at the UB Supersite so it can be concluded that the measured concentrations at the UB Supersite correspond to urban background concentrations in Helsinki area.

Concentration of total particulate organics and secondary organics showed similar increase during the three episodes at the UB Supersite and Traffic Supersite (Fig. S6). The increased $PM_{2.5}$ concentration during episodes is connected to formation of secondary particulate matter together with increased concentration of total organic matter. During non-episodic periods concentration of total particulate organics was higher at the Traffic Supersite compared to the UB Supersite indicating that it had a local source, most probably traffic, at the Traffic Supersite.

During all episode periods the concentration of $PM_{2.5}$ and LDSA (Fig. S2, Table 1 and S3) and BC (Traffic Supersite and UB Supersite, Fig. 6) together with biomass burning tracer levoglucosan and sum of measured polycyclic hydrocarbons (PAH, Traffic Supersite) showed clear increase in their concentrations. It seems that the long-range or regional transported air masses contained of particles originated form biomass burning and that the transported particles clearly increased the $PM_{2.5}$ and BC concentrations and so degrading the air quality in Helsinki area. The increased LDSA concentrations during these episodes further degrade the air quality in Helsinki Metropolitan area. During cold season wood burning for heating purposes especially in detached house areas in Helsinki takes place. However, the effect of local wood burning on pollutant concentrations at the Traffic Supersite is minimal on annual level compared to the effect of traffic related pollutants (Aurela et al., 2015; Helin et al., 2021; Kangas et al., 2024). This can be seen also from the relatively low concentration of levoglucosan and sum of measured PAH's during non-episodic period. However, the concentration of

https://doi.org/10.5194/egusphere-2024-2235
Preprint. Discussion started: 7 October 2024

levoglucosan and PAHs increased during the episodes indicating that long-range or regionally transported biomass burning aerosol was transported to the measurement site.

Fig. S7 shows the particle number size distributions at the Traffic Supersite and UB Supersite during the three episodes and during the traffic related (non-episodic) period. The mean particle number concentration did not show any marked increase during the episodes compared to non-episodic situation at Supersite, but the mean LDSA concentrations measured with AQ Urban instrument were clearly higher. The increased LDSA concentration during the episodes is connected to higher concentration of larger particles at both sites (Fig. S7). The higher LDSA concentration at the Traffic Supersite compared to the UB Supersite during non-episodic situation is due to higher concentration of traffic related ultrafine particles at the Traffic Supersite.

HYSPLIT back trajectories were calculated during these episodes on daily basis (3-hour resolution, 96-hour back trajectories, Fig. S8). The air masses during the short period E1 came from Arctic areas. The air masses during the E2 period between 31 January and 3 February came from Eastern Europe (Moscow area, Fig. S8) straight to the measurement site and between 4 February and 5 February came across Baltia and Belarus. During the E3 period the airmasses circulated first over Central Europe (Poland and Baltia, 13–14 February) and then arrived from Southern Europe over Romania, Ukraine, Belarus, Poland and Baltia.

The coldest temperatures during the measurement campaign were measured during periods E1 and E2 (Fig. 2) and only during the period E3 the temperature was near 0 °C. It is possible that especially traffic related particulate component and trace gases also accumulated in the boundary layer during the cold days and that the increased concentrations are due both this accumulation and long-range transported pollutants. The concentrations of traffic related gaseous pollutants CO, CO_2, NO, and NO_2 showed higher concentrations at the Traffic Supersite (Table 1) during episodes compared to non-episodic period, especially during the long-lasting episode E2 when also the wind speed was very low at the last days of this episode. For CO_2 this increase was minimal and for PN concentration only slight difference between episodes and workdays without episodes could be seen. Clearer was the difference of PN concentration between non episodic workdays and weekends (Table 1).

3.1.6 Source apportionment of organics in aerosol particles

A source apportionment of organics was performed for the AMS data obtained from the Traffic Supersite. As observed in Fig. S9 and S10, the obtained solution consisted of 6 factors: OA with a significant signal at m/z 60 ($C_2H_4O_2^+$) and 61 ($C_2H_5O_2^+$), Tr-OOA; low-volatility oxygenated OA (LV-OOA) with a large signal at m/z 44 (CO_2^+); hydrocarbon-like OA (HOA) mostly composed of $C_XH_Y^+$ fragments; biomass burning OA (BBOA) with characteristic m/z 60 ($C_2H_4O_2^+$) and m/z 73 ($C_3H_5O_2^+$) signal peaks; semi-volatile oxygenated OA (SV-OOA) with high signal at m/z 43 ($C_2H_3O^+$); and LV-OOA-BB that had also a high signal at m/z 44 but as well a significant signal at m/z 60.

The share of chemical composition of major measured compounds (BC, organics, sulphate, nitrate, ammonium, and chloride) as well as the share of organic factors are shown in Fig. S11. Concerning primary emissions, HOA was the dominant factor at the traffic site, with an average contribution of 12.5 % during the whole campaign period Fig. S11. In fact, HOA had a good correlation with NO and NO_2 (R^2 equal to 0.82 and 0.87, respectively) and was particularly high

https://doi.org/10.5194/egusphere-2024-2235
Preprint. Discussion started: 7 October 2024

during workdays and traffic rush hours (Table 1 and Fig. S11). This evidence shows the predominant contribution from traffic to this factor. On the other hand, the overall contribution from BBOA was small (6.1%), even though the mean concentration of BBOA was like the one of HOA during weekends. This low BBOA contribution reflects the fact that residences around the measurement site do not use biomass burning as a dominant heating source (e.g. Kangas et al., 2024 and Barreira et al., 2021) The obtained results agree with previous observations at the same measurement site concerning primary organic aerosol chemical characteristics during wintertime (Lepistö et al., 2023b).

Contrary to primary emissions, SV-OOA, LV-OOA, and LV-OOA-BB, which mostly represent secondary organic emissions, constituted on average 67.7 % of the total organics during the campaign period (Table 1 and Fig. S11). The concentration of LV-OOA-BB factor was especially high during the E1, E2 and E3 periods reaching up to 52.8, 47.4, and 56.2% for the forementioned periods, respectively indicating a strong influence of long range transported aerosol during these periods. These results reveal the high importance of long-range transport episodes to the atmospheric particulate mass and composition in Helsinki. Furthermore, they suggest a heterogenicity of chemical and physical properties of long-range transported particles because of distinct production and emission sources. Interestingly, the SV-OOA contribution was relatively constant during all events (approximately 15%), except in E3 due to the increased contribution from LV-OOA-BB (lower SV-OOA contribution). SV-OOA is expected to be low during winter due to decreased atmospheric photochemistry comparatively to the warmest periods of the year (e.g. Praplan et al., 2017).

During episodes E2 and E3, all factors derived from the PMF analysis exhibited heightened concentrations, including the HOA factor known to stem from local traffic emissions. This result suggests that, during these episodes, aerosol particles comprised a blend of both transported and locally emitted pollutants, despite the dominance of LV-OOA aerosol.

3.1.7 Traffic related (non-episodic) period

Table 1 shows the mean traffic frequencies and concentrations of gaseous and particulate pollutants at the Traffic Supersite during traffic related (non-episodic) period divided further as workdays and weekends and during the three periods with high pollutant concentrations.

The traffic frequency during workdays was on average 1.4 times higher than during the weekends which is mostly due to the lack of commuter traffic during weekends. Probably the number of trucks and other heavy-duty vehicles during the weekends is also smaller. The mean concentrations of PN, NO, NO_2, BC, $PM_{2.5-10}$, and HOA were higher during the workdays compared to weekends, which is expected since PN, NO, NO_2, BC, and HOA are emitted directly from motor engines. Local traffic also increases concentration of coarse particles, but their concentration also depends on meteorology like rain, snow cover, or wind speed. Concentrations of most pollutants decreased with increasing wind speed despite of the wind direction.

Mean LDSA concentration is connected to both PN concentration and particle size. The lower mean PN concentration together with lower mean LDSA concentrations during non-episodic weekends indicates that LDSA concentration is connected to local PN emissions during non-episodic period. The effect of long-range or regionally transported aerosol to the LDSA concentration is clearly stronger than the effect of local traffic during the episodes. However, in general the local traffic related PN emissions dominate the LDSA concentration at the Traffic Supersite which can be seen on the

https://doi.org/10.5194/egusphere-2024-2235
Preprint. Discussion started: 7 October 2024

higher LDSA concentration during the daytime at the Traffic Supersite compared to the UB Supersite (Fig. S12). The slightly higher mean concentration of total organics during the workdays is probably due to the higher HOA concentrations during workdays.

The hourly variations of PN, BC, NO_x, $PM_{2.5}$, $PM_{2.5-10}$, and LDSA during non-episodic period are shown in Fig. S12 (workdays) and Fig. S13 (weekends) at the Traffic Supersite and UB Supersite station. During workdays the hourly variations of PN, BC, NO_x and LDSA are clearly connected to local traffic frequencies (Fig. 2 and Fig. S12) showing the morning and late afternoon rush hours. The concentrations of $PM_{2.5}$ and $PM_{2.5-10}$ also increased during daytime but were not as clearly correlated to morning and afternoon rush hours. Their concentrations started to rise during morning hours and stayed high during the daytime. The hourly variations of these compounds were similar at the UB Supersite, but their concentrations were much lower.

The hourly variations of total organics and the calculated factors HOA, BBOA, SV-OOA, LV-OOA, LV-OOA-BB, and Tr-OOA during non-episodic period are shown in Fig. S14 (workdays) and Fig. S15 (weekends). The hourly variation of HOA factor is clearly connected to traffic frequencies and the increased concentration of total organics can be explained majority with the increase in HOA concentration. The factor connected to biomass burning (BBOA) shows two peaks one in midday and another in evening. The evening peak is probably connected to wood burning in Helsinki area. Wood burning takes places in detached houses in Helsinki in sauna stoves and housewarming purposes especially during cold months. During weekends no clear traffic dependences of HOA and total organics could be seen. The evening peak of BBOA was clearly seen also during weekends and it started already after late afternoon which is due to more active use of sauna stoves and fireplaces during weekends. The diurnal cycle of Tr-OOA during workdays (Fig S14) indicates that it was connected to local traffic related emissions.

3.1.8 Local pollution level comparison – CPCs and PDA

CPCs number concentration time series were used to compare local pollution level differences at the Traffic Supersite and the UB Supersite stations. It can be seen from the time series (Fig. S16) that significantly higher particle concentration levels are frequently observed at the Traffic Supersite during the campaign. To look at the differences between the sites in more detail, we employed the pollution detection algorithm (PDA, Beck et al., 2022). The PDA identifies and flags polluted periods in five steps, most importantly by the first filter step: the time derivative (gradient) of a concentration over time.

PDA is primarily designed to identify and flag periods of polluted data in remote atmospheric composition time series, but it might also be applied to locations where local contamination interference is so frequent that most data points exceed the contribution from the underlying background in the period of interest, like in urban areas (Beck et al., 2022). PDA only relies on the concentration time series datasets and is independent of ancillary datasets, such as meteorological variables or black carbon data. Consequently, the PDA can provide valuable additional information on the pollution levels and characteristics of urban conditions.

Fig. 7 and Fig. S17 show PDA filter results for the Traffic Supersite and the UB Supersite for the campaign period by using typical PDA parameters for the 1 min time resolution data (Beck et al., 2022). CPC data gaps (Fig S17), 1.3 % and

https://doi.org/10.5194/egusphere-2024-2235
Preprint. Discussion started: 7 October 2024

6.6 % of the Traffic Supersite and UB Supersite, respectively, were assigned to one and removed for CPC total counts (Table 2). It should be noted that although both CPCs were operational simultaneously most of the time during the campaign, these data gaps cause some uncertainty in the analysis. Identical PDA settings were used for both stations. Interquartile range (IQR) filter, instead of power law derivative filter was used as a first derivative filter as it is better suited for the current (relatively polluted) urban data with no clear separation of data to polluted/unpolluted branches. We compared two cases, one with threshold filter for typical polluted concentration levels > 10^4 p cm^{-3}, (Fig. S17) and with the upper threshold set to 3×10^5 p cm^{-3} (upper concentration range of the measurements) to observe differences in the derivative filtering without threshold filter that otherwise dominates in the urban environment (Fig 7). It can be seen that the flagged (red) data fraction is more prominent in Traffic Supersite data. All employed filter steps and PDA parameters are shown in Tables S4 and S5.

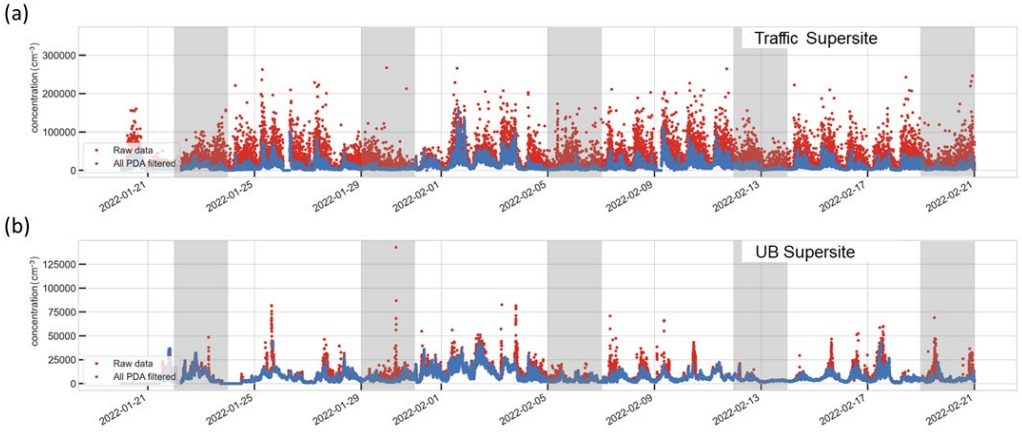

Figure 7. PDA filter results for the Traffic Supersite (a) and the UB Supersite (b) after identical filtering steps, showing the flagged data (red) with the threshold set to upper concentration range of the measurements. Shadowed periods represent weekends. See Table S5 for the applied filter steps and parameters.

The PDA results are summarized in Table 2. In both cases, the ratio of the PDA filtered data for Traffic Supersite/UB Supersite was similar (1.9 and 2.0). The higher pollution ratio for the case without the upper threshold filter (gradient filter dominates), seems to reflect more polluted conditions due to local traffic and near roadside conditions at the Traffic Supersite as the higher derivatives are representing periods of high concentration variability, i.e., due to local source (Beck et al., 2022).

https://doi.org/10.5194/egusphere-2024-2235
Preprint. Discussion started: 7 October 2024

Table 2. An overview of the PDA results and percentage of data declared as polluted with the applied filtering steps.

	Traffic Supersite (number of data points)	**UB Supersite (number of data points)**	**Traffic Supersite (%)**	**UB Supersite (%)**	**Ratio Traffic Supersite/UB Supersite**
Total counts (number of data points).	46915	44383			
PDA polluted (10 000 p cm^{-3} threshold), Fig. S17.	33023	16463	**70.4**	**37.1**	**1.9**
PDA polluted (no threshold, >300 000 p cm^{-3}), Fig. 7.	16638	7985	**35.5**	**18.0**	**2.0**

3.1.9 NAIS particle size distribution comparison

Fig. 8 presents hourly median particle size distributions obtained during the workdays (Monday–Friday) with the NAIS particle mode, negative polarity at the Traffic Supersite (Fig. 8a) and at the UB Supersite (Fig. 8b). It is clear also from the NAIS measurements that the Traffic Supersite location has significantly higher median particle concentrations throughout the day, starting from the early working hours (~ 6:00) and continuing to late evening (22:00). Furthermore, it appears that during office hours the relatively high particle concentrations (~ 10^4 p cm^{-3}) are observed also at the sub-3 nm size range and lower size range of nucleation mode (3–5 nm), whereas at the UB Supersite similar concentrations are observed only for particles > 5 nm. At UB Supersite the sub-5 nm particle concentrations are also rapidly decreasing after ~ 17:00, while at the Traffic Supersite the concentrations remain relatively high until ~ 22:00.

https://doi.org/10.5194/egusphere-2024-2235
Preprint. Discussion started: 7 October 2024

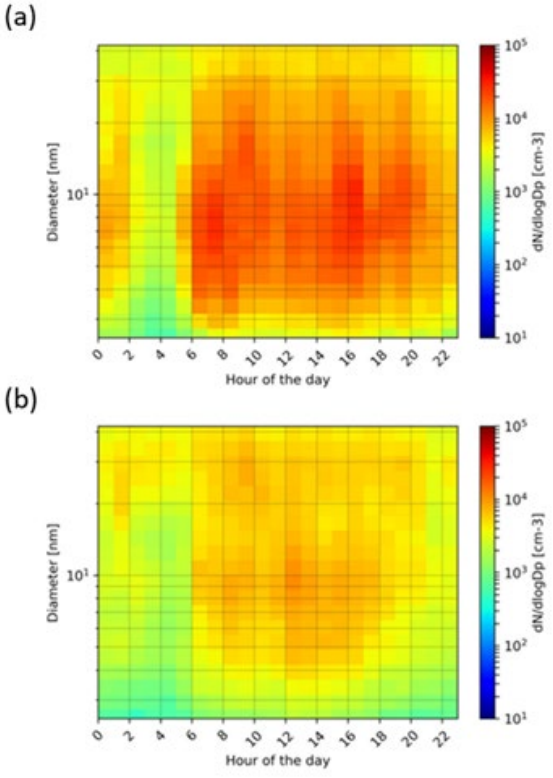

Figure 8. Hourly median particle size distributions obtained from NAIS negative polarity during the campaign workdays (Monday–Friday) at the Traffic Supersite (a) and the corresponding particle size distributions at the UB Supersite (b).

Data Availability

Data described in this manuscript can be accessed at Zenodo repository under DOI 10.5281/zenodo.13254916 (Teinilä, 2024).

4 Conclusions

In this study physical and chemical properties of particulate matter and concentrations of trace gases were measured at an urban traffic site in Helsinki, Finland. The five-week intensive campaign took place at the Traffic Supersite in Helsinki in January–February 2022. The goal of the study was to characterise wintertime aerosol and obtain information on factors affecting air quality at urban traffic site in wintertime. To estimate the importance of local traffic and long-range transported pollutants on the air quality, measurements were made same time also at an urban background Supersite. A source apportionment of organics was performed for the SP-AMS measurements at the Traffic Supersite. The solution consisted of five factors three connected to primary emissions (HOA, BBOA, and Tr-OOA) and three to aged aerosol (SV-OOA, LV-OOA and LV-OOA-BB).

During the intensive campaign the meteorological conditions such as temperature, snow cover, and rain varied largely. Three clear pollution episodes with elevated concentrations of particulate matter and trace gases took place during the campaign. During these episodes the increased pollutant concentrations were connected to trapping of local pollutants on

https://doi.org/10.5194/egusphere-2024-2235
Preprint. Discussion started: 7 October 2024

the boundary layer and long- and regional range transport of pollutants to the site. The concentrations of traffic related pollutants PN, NO, NO_2, BC, and HOA followed the traffic frequencies on an hourly basis and having also lower concentrations during weekends when traffic frequencies were lower. The source apportionment showed that, in addition to traffic related primary HOA, particulate matter consisted also biomass burning related aerosol (BBOA factor). During the pollution episodes high concentrations of secondary inorganics (sulphate, nitrate, and ammonium) and secondary organics (SV-OOA, LV-OOA, and LV-OOA-BB) were observed. Especially the concentration of secondary organics containing biomass burning material, LV-OOA-BB was very high, showing concentrations as high as 6 $\mu g\ m^{-3}$ and it was the dominant factor during episodes E1, E2 and E3. This together with the increased concentration of levoglucosan and BC indicate that long-range or regionally transported aerosol contained biomass burning originated particles.

The pollutant concentrations were affected also by meteorology like wind speed and temperature. During cold periods especially pollutants from local traffic trapped on the boundary layer increasing their concentrations. Stagnant conditions with low wind speed during coldest days inhibit the ventilation and removal of local pollutants effectively. Concentrations of most pollutants decreased with increasing wind speed.

It can be concluded that the air quality at the Traffic Supersite was affected by both changes in pollution sources and removal of pollutants. The two most important pollution sources at the site were local traffic and long-range or regional transportation. Long-range or regional transported aerosol is present constantly in the Helsinki area, but we also observed episodes with markedly increased pollutant concentrations and increased $PM_{2.5}$ concentrations. During these episodes $PM_{2.5}$ mainly consisted of secondary inorganic and organic aerosol and black carbon. Trapping of pollutants with stagnant conditions during coldest days also increased pollutant concentrations originated from local traffic exhaust. As long-range transported pollutant episodes increased $PM_{2.5}$ mass, the pollutants from local traffic increased particle number concentration. The effect of local traffic on particle number concentration was most clearly seen in diurnal variation of PN with morning and afternoon rush hours and lowered PN concentration during weekends. A strong effect of traffic was seen also with the concentrations of the smallest nanoparticles (both < 5 nm and < 10 nm) which agrees with existing literature. As expected, due to traffic as a major local source, aromatic hydrocarbons made the highest contribution to the total measured concentration of SOA precursor VOCs (> C5).

The fact that we observed such a high contribution of long-range and regionally transported pollutants to PM mass and concentration of secondary inorganic and organic constituents show the need to tackle atmospheric pollutants not only at local level, but in concerted actions involving regional and international regulative entities.

Competing interests

At least one of the (co-)authors is a member of the editorial board of Atmospheric Chemistry and Physics.

Acknowledgments

Long-term research co-operation and support from HSY to this project is gratefully acknowledged. Katja Moilanen from the City of Helsinki is acknowledged for the traffic count data. Financial support from Black Carbon Footprint project funded by Business Finland and participating companies (Grant 528/31/2019), from Technology Industries of Finland Centennial Foundation to Urban Air Quality 2.0 project, EU Horizon 2020 Framework Programme via the Research Infrastructures Services Reinforcing Air Quality Monitoring Capacities in European Urban & Industrial AreaS (RI-

https://doi.org/10.5194/egusphere-2024-2235
Preprint. Discussion started: 7 October 2024

URBANS) project (GA-101036245) and Academy of Finland project BBrCaC (grant no. 341271) as well as Flagship ACCC (grant no. 337552, 337551) are gratefully acknowledged. This work was supported by the Finnish Research Impact Foundation under grant 4708620.

https://doi.org/10.5194/egusphere-2024-2235
Preprint. Discussion started: 7 October 2024

References

Amanatidis, S., Ntziachristos, L., Karjalainen, P., Saukko, E., Simonen, P., Kuittinen, N., Aakko-Saksa, P., Timonen, H., Rönkkö, T., and Keskinen, J.: Comparative performance of a thermal denuder and a catalytic stripper in sampling laboratory and marine exhaust aerosols, Aerosol Sci. Technol., 52, 420–432, https://doi.org/10.1080/02786826.2017.1422236, 2018.

Atkinson, R. W., Kang, S., Anderson, H. R., Mills, I. C., and Walton, H. A.: Epidemiological time series studies of $PM_{2.5}$ and daily mortality and hospital admissions: a systematic review and meta-analysis, Thorax, 69, 660–665, https://doi.org/10.1136/thoraxjnl-2013-204492, 2014.

Aurela, M., Saarikoski, S., Niemi, J. V., Canonaco, F., Prevot, A. S. H., Frey, A., Carbone, S., Kousa, A., and Hillamo, R.: Chemical and Source Characterization of Submicron Particles at Residential and Traffic Sites in the Helsinki Metropolitan Area, Finland, Aerosol Air Qual. Res., 15, 1213–1226, https://doi.org/10.4209/aaqr.2014.11.0279, 2015.

Barreira, L. M. F., Helin, A., Aurela, M., Teinilä, K., Friman, M., Kangas, L., Niemi, J. V., Portin, H., Kousa, A., Pirjola, L., Rönkkö, T., Saarikoski, S., and Timonen, H.: In-depth characterization of submicron particulate matter inter-annual variations at a street canyon site in northern Europe, Atmospheric Chem. Phys., 21, 6297–6314, https://doi.org/10.5194/acp-21-6297-2021, 2021.

Beck, I., Angot, H., Baccarini, A., Dada, L., Quéléver, L., Jokinen, T., Laurila, T., Lampimäki, M., Bukowiecki, N., Boyer, M., Gong, X., Gysel-Beer, M., Petäjä, T., Wang, J., and Schmale, J.: Automated identification of local contamination in remote atmospheric composition time series, Atmospheric Meas. Tech., 15, 4195–4224, https://doi.org/10.5194/amt-15-4195-2022, 2022.

Birch, M. E. and Cary, R. A.: Elemental Carbon-Based Method for Monitoring Occupational Exposures to Particulate Diesel Exhaust, Aerosol Sci. Technol., 25, 221–241, https://doi.org/10.1080/02786829608965393, 1996.

Canagaratna, M. R., Jimenez, J. L., Kroll, J. H., Chen, Q., Kessler, S. H., Massoli, P., Hildebrandt Ruiz, L., Fortner, E., Williams, L. R., Wilson, K. R., Surratt, J. D., Donahue, N. M., Jayne, J. T., and Worsnop, D. R.: Elemental ratio measurements of organic compounds using aerosol mass spectrometry: characterization, improved calibration, and implications, Atmospheric Chem. Phys., 15, 253–272, https://doi.org/10.5194/acp-15-253-2015, 2015.

Canonaco, F., Crippa, M., Slowik, J. G., Baltensperger, U., and Prévôt, A. S. H.: SoFi, an IGOR-based interface for the efficient use of the generalized multilinear engine (ME-2) for the source apportionment: ME-2 application to aerosol mass spectrometer data, Atmospheric Meas. Tech., 6, 3649–3661, https://doi.org/10.5194/amt-6-3649-2013, 2013.

Carbone, S., Aurela, M., Saarnio, K., Saarikoski, S., Timonen, H., Frey, A., Sueper, D., Ulbrich, I. M., Jimenez, J. L., Kulmala, M., Worsnop, D. R., and Hillamo, R. E.: Wintertime Aerosol Chemistry in Sub-Arctic Urban Air, Aerosol Sci. Technol., 48, 313–323, https://doi.org/10.1080/02786826.2013.875115, 2014.

Carslaw, D. C. and Ropkins, K.: openair — An R package for air quality data analysis, Environ. Model. Softw., 27–28, 52–61, https://doi.org/10.1016/j.envsoft.2011.09.008, 2012.

Cavalli, F., Viana, M., Yttri, K. E., and Genberg, J.: Toward a standardised thermal-optical protocol for measuring atmospheric organic and elemental carbon: the EUSAAR protocol, Atmos Meas Tech, 2010.

Coggon, M. M., Gkatzelis, G. I., McDonald, B. C., Gilman, J. B., Schwantes, R. H., Abuhassan, N., Aikin, K. C., Arend, M. F., Berkoff, T. A., Brown, S. S., Campos, T. L., Dickerson, R. R., Gronoff, G., Hurley, J. F., Isaacman-VanWertz, G., Koss, A. R., Li, M., McKeen, S. A., Moshary, F., Peischl, J., Pospisilova, V., Ren, X., Wilson, A., Wu, Y., Trainer, M., and Warneke, C.: Volatile chemical product emissions enhance ozone and modulate urban chemistry, Proc. Natl. Acad. Sci., 118, e2026653118, https://doi.org/10.1073/pnas.2026653118, 2021.

Drinovec, L., Močnik, G., Zotter, P., Prévôt, A. S. H., Ruckstuhl, C., Coz, E., Rupakheti, M., Sciare, J., Müller, T., Wiedensohler, A., and Hansen, A. D. A.: The "dual-spot" Aethalometer: an improved measurement of aerosol black carbon with real-time loading compensation, Atmospheric Meas. Tech., 8, 1965–1979, https://doi.org/10.5194/amt-8-1965-2015, 2015.

Gentner, D. R., Jathar, S. H., Gordon, T. D., Bahreini, R., Day, D. A., El Haddad, I., Hayes, P. L., Pieber, S. M., Platt, S. M., de Gouw, J., Goldstein, A. H., Harley, R. A., Jimenez, J. L., Prévôt, A. S. H., and Robinson, A. L.: Review of

https://doi.org/10.5194/egusphere-2024-2235
Preprint. Discussion started: 7 October 2024

Urban Secondary Organic Aerosol Formation from Gasoline and Diesel Motor Vehicle Emissions, Environ. Sci. Technol., 51, 1074–1093, https://doi.org/10.1021/acs.est.6b04509, 2017.

Hansen, A. D. A., Rosen, H., and Novakov, T.: The aethalometer — An instrument for the real-time measurement of optical absorption by aerosol particles, Carbonaceous Part. Atmosphere 1983, 36, 191–196, https://doi.org/10.1016/0048-9697(84)90265-1, 1984.

Heikkilä, J., Rönkkö, T., Lähde, T., Lemmetty, M., Arffman, A., Virtanen, A., Keskinen, J., Pirjola, L., and Rothe, D.: Effect of Open Channel Filter on Particle Emissions of Modern Diesel Engine, J. Air Waste Manag. Assoc., 59, 1148–1154, https://doi.org/10.3155/1047-3289.59.10.1148, 2009.

Helin, A., Virkkula, A., Backman, J., Pirjola, L., Sippula, O., Aakko-Saksa, P., Väätäinen, S., Mylläri, F., Järvinen, A., Bloss, M., Aurela, M., Jakobi, G., Karjalainen, P., Zimmermann, R., Jokiniemi, J., Saarikoski, S., Tissari, J., Rönkkö, T., Niemi, J. V., and Timonen, H.: Variation of Absorption Ångström Exponent in Aerosols From Different Emission Sources, J. Geophys. Res. Atmospheres, 126, https://doi.org/10.1029/2020JD034094, 2021.

Hellén, H., Tykkä, T., and Hakola, H.: Importance of monoterpenes and isoprene in urban air in northern Europe, Atmos. Environ., 59, 59–66, https://doi.org/10.1016/j.atmosenv.2012.04.049, 2012.

Hietikko, R., Kuuluvainen, H., Harrison, R. M., Portin, H., Timonen, H., Niemi, J. V., and Rönkkö, T.: Diurnal variation of nanocluster aerosol concentrations and emission factors in a street canyon, Atmos. Environ., 189, 98–106, https://doi.org/10.1016/j.atmosenv.2018.06.031, 2018.

Järvi, L., Junninen, H., Karppinen, A., Hillamo, R., Virkkula, A., Mäkelä, T., Pakkanen, T., and Kulmala, M.: Temporal variations in black carbon concentrations with different time scales in Helsinki during 1996–2005, Atmospheric Chem. Phys., 8, 1017–1027, https://doi.org/10.5194/acp-8-1017-2008, 2008.

Järvi, L., Hannuniemi, H., Hussein, T., Junninen, H., Aalto, P., Hillamo, R., Mäkelä, T., Keronen, P., Siivola, E., Vesala, T., and Kulmala, M.: The urban measurement station SMEAR III: Continuous monitoring of air pollution and surface–atmosphere interactions in Helsinki, Finland, 14, n.d.

Järvi, L., Hannuniemi, H., Hussein, T., Junninen, H., Aalto, P., Hillamo, R., Mäkelä, T., Keronen, P., Siivola, E., Vesala, T., and Kulmala, M.: The urban measurement station SMEAR III: Continuous monitoring of air pollution and surface–atmosphere interactions in Helsinki, Finland, 14, n.d.

Järvinen, A., Aitomaa, M., Rostedt, A., Keskinen, J., and Yli-Ojanperä, J.: Calibration of the new electrical low pressure impactor (ELPI+), J. Aerosol Sci., 69, 150–159, https://doi.org/10.1016/j.jaerosci.2013.12.006, 2014.

Kangas, L., Kukkonen, J., Kauhaniemi, M., Riikonen, K., Sofiev, M., Kousa, A., Niemi, J. V., and Karppinen, A.: The contribution of residential wood combustion to the $PM_{2.5}$ concentrations in the Helsinki metropolitan area, Atmospheric Chem. Phys., 24, 1489–1507, https://doi.org/10.5194/acp-24-1489-2024, 2024.

Karppinen, A., Joffre, S. M., and Kukkonen, J.: The refinement of a meteorological pre-processor for the urban environment, Int. J. Environ. Pollut., 14, 565–572, https://doi.org/10.1504/IJEP.2000.000580, 2000.

Keskinen, J., Pietarinen, K., and Lehtimäki, M.: Electrical low pressure impactor, J. Aerosol Sci., 23, 353–360, https://doi.org/10.1016/0021-8502(92)90004-F, 1992.

Kuula, J., Kuuluvainen, H., Niemi, J. V., Saukko, E., Portin, H., Kousa, A., Aurela, M., Rönkkö, T., and Timonen, H.: Long-term sensor measurements of lung deposited surface area of particulate matter emitted from local vehicular and residential wood combustion sources, Aerosol Sci. Technol., 54, 190–202, https://doi.org/10.1080/02786826.2019.1668909, 2020.

Kuuluvainen, H., Poikkimäki, M., Järvinen, A., Kuula, J., Irjala, M., Dal Maso, M., Keskinen, J., Timonen, H., Niemi, J. V., and Rönkkö, T.: Vertical profiles of lung deposited surface area concentration of particulate matter measured with a drone in a street canyon, Environ. Pollut., 241, 96–105, https://doi.org/10.1016/j.envpol.2018.04.100, 2018.

Lampimäki, M., Baalbaki, R., Ahonen, L., Korhonen, F., Cai, R., Chan, T., Stolzenburg, D., Petäjä, T., Kangasluoma, J., Vanhanen, J., and Lehtipalo, K.: Novel aerosol diluter – Size dependent characterization down to 1 nm particle size, J. Aerosol Sci., 172, 106180, https://doi.org/10.1016/j.jaerosci.2023.106180, 2023.

https://doi.org/10.5194/egusphere-2024-2235
Preprint. Discussion started: 7 October 2024

Leino, K., Riuttanen, L., Nieminen, T., Maso, M. D., Väänänen, R., Pohja, T., Keronen, P., Järvi, L., Aalto, P. P., Virkkula, A., Kerminen, V.-M., Petäjä, T., and Kulmala, M.: Biomass-burning smoke episodes in Finland from eastern European wildfires, 19, n.d.

Lelieveld, J., Evans, J. S., Fnais, M., Giannadaki, D., and Pozzer, A.: The contribution of outdoor air pollution sources to premature mortality on a global scale, Nature, 525, 367–371, https://doi.org/10.1038/nature15371, 2015.

Lepistö, T., Kuuluvainen, H., Juuti, P., Järvinen, A., Arffman, A., and Rönkkö, T.: Measurement of the human respiratory tract deposited surface area of particles with an electrical low pressure impactor, Aerosol Sci. Technol., 54, 958–971, https://doi.org/10.1080/02786826.2020.1745141, 2020.

Lepistö, T., Lintusaari, H., Oudin, A., Barreira, L. M. F., Niemi, J. V., Karjalainen, P., Salo, L., Silvonen, V., Markkula, L., Hoivala, J., Marjanen, P., Martikainen, S., Aurela, M., Reyes, F. R., Oyola, P., Kuuluvainen, H., Manninen, H. E., Schins, R. P. F., Vojtisek-Lom, M., Ondracek, J., Topinka, J., Timonen, H., Jalava, P., Saarikoski, S., and Rönkkö, T.: Particle lung deposited surface area (LDSAal) size distributions in different urban environments and geographical regions: Towards understanding of the PM2.5 dose–response, Environ. Int., 180, 108224, https://doi.org/10.1016/j.envint.2023.108224, 2023a.

Lepistö, T., Barreira, L. M. F., Helin, A., Niemi, J. V., Kuittinen, N., Lintusaari, H., Silvonen, V., Markkula, L., Manninen, H. E., Timonen, H., Jalava, P., Saarikoski, S., and Rönkkö, T.: Snapshots of wintertime urban aerosol characteristics: Local sources emphasized in ultrafine particle number and lung deposited surface area, Environ. Res., 231, 116068, https://doi.org/10.1016/j.envres.2023.116068, 2023b.

Lintusaari, H., Kuuluvainen, H., Vanhanen, J., Salo, L., Portin, H., Järvinen, A., Juuti, P., Hietikko, R., Teinilä, K., Timonen, H., Niemi, J. V., and Rönkkö, T.: Sub-23 nm Particles Dominate Non-Volatile Particle Number Emissions of Road Traffic, Environ. Sci. Technol., 57, 10763–10772, https://doi.org/10.1021/acs.est.3c03221, 2023.

Liu, P. S. K., Deng, R., Smith, K. A., Williams, L. R., Jayne, J. T., Canagaratna, M. R., Moore, K., Onasch, T. B., Worsnop, D. R., and Deshler, T.: Transmission Efficiency of an Aerodynamic Focusing Lens System: Comparison of Model Calculations and Laboratory Measurements for the Aerodyne Aerosol Mass Spectrometer, Aerosol Sci. Technol., 41, 721–733, https://doi.org/10.1080/02786820701422278, 2007.

Liu, X., Hadiatullah, H., Zhang, X., Trechera, P., Savadkoohi, M., Garcia-Marlès, M., Reche, C., Pérez, N., Beddows, D. C. S., Salma, I., Thén, W., Kalkavouras, P., Mihalopoulos, N., Hueglin, C., Green, D. C., Tremper, A. H., Chazeau, B., Gille, G., Marchand, N., Niemi, J. V., Manninen, H. E., Portin, H., Zikova, N., Ondracek, J., Norman, M., Gerwig, H., Bastian, S., Merkel, M., Weinhold, K., Casans, A., Casquero-Vera, J. A., Gómez-Moreno, F. J., Artíñano, B., Gini, M., Diapouli, E., Crumeyrolle, S., Riffault, V., Petit, J.-E., Favez, O., Putaud, J.-P., Santos, S. M. D., Timonen, H., Aalto, P. P., Hussein, T., Lampilahti, J., Hopke, P. K., Wiedensohler, A., Harrison, R. M., Petäjä, T., Pandolfi, M., Alastuey, A., and Querol, X.: Ambient air particulate total lung deposited surface area (LDSA) levels in urban Europe, Sci. Total Environ., 898, 165466, https://doi.org/10.1016/j.scitotenv.2023.165466, 2023.

Manninen, H. E., Mirme, S., Mirme, A., Petäjä, T., and Kulmala, M.: How to reliably detect molecular clusters and nucleation mode particles withNeutral cluster and Air Ion Spectrometer (NAIS), Atmospheric Meas. Tech., 9, 3577–3605, https://doi.org/10.5194/amt-9-3577-2016, 2016.

Marjamäki, M., Keskinen, J., Chen, D.-R., and Pui, D. Y. H.: PERFORMANCE EVALUATION OF THE ELECTRICAL LOW-PRESSURE IMPACTOR (ELPI), J. Aerosol Sci., 31, 249–261, https://doi.org/10.1016/S0021-8502(99)00052-X, 2000.

Marques, B., Kostenidou, E., Valiente, A. M., Vansevenant, B., Sarica, T., Fine, L., Temime-Roussel, B., Tassel, P., Perret, P., Liu, Y., Sartelet, K., Ferronato, C., and D'Anna, B.: Detailed Speciation of Non-Methane Volatile Organic Compounds in Exhaust Emissions from Diesel and Gasoline Euro 5 Vehicles Using Online and Offline Measurements, Toxics, 10, 184, https://doi.org/10.3390/toxics10040184, 2022.

Mirme, S. and Mirme, A.: The mathematical principles and design of the NAIS – a spectrometer for the measurement of cluster ion and nanometer aerosol size distributions, Atmospheric Meas. Tech., 6, 1061–1071, https://doi.org/10.5194/amt-6-1061-2013, 2013.

Ng, N. L., Herndon, S. C., Trimborn, A., Canagaratna, M. R., Croteau, P. L., Onasch, T. B., Sueper, D., Worsnop, D. R., Zhang, Q., Sun, Y. L., and Jayne, J. T.: An Aerosol Chemical Speciation Monitor (ACSM) for Routine Monitoring

https://doi.org/10.5194/egusphere-2024-2235
Preprint. Discussion started: 7 October 2024

of the Composition and Mass Concentrations of Ambient Aerosol, Aerosol Sci. Technol., 45, 780–794, https://doi.org/10.1080/02786826.2011.560211, 2011.

Niemi, J. V., Tervahattu, H., Vehkamäki, H., Kulmala, M., Koskentalo, T., Sillanpää, M., and Rantamäki, M.: Characterization and source identification of a fine particle episode in Finland, Atmos. Environ., 38, 5003–5012, https://doi.org/10.1016/j.atmosenv.2004.06.023, 2004.

Niemi, J. V., Tervahattu, H., Vehkamäki, H., Martikainen, J., Laakso, L., Kulmala, M., Aarnio, P., Koskentalo, T., Sillanpää, M., and Makkonen, U.: Characterization of aerosol particle episodes in Finland caused by wildfires in Eastern Europe, Atmospheric Chem. Phys., 5, 2299–2310, https://doi.org/10.5194/acp-5-2299-2005, 2005.

Niemi, J. V., Saarikoski, S., Aurela, M., Tervahattu, H., Hillamo, R., Westphal, D. L., Aarnio, P., Koskentalo, T., Makkonen, U., Vehkamäki, H., and Kulmala, M.: Long-range transport episodes of fine particles in southern Finland during 1999–2007, Atmos. Environ., 43, 1255–1264, https://doi.org/10.1016/j.atmosenv.2008.11.022, 2009.

Okuljar, M., Kuuluvainen, H., Kontkanen, J., Garmash, O., Olin, M., Niemi, J. V., Timonen, H., Kangasluoma, J., Tham, Y. J., Baalbaki, R., Sipilä, M., Salo, L., Lintusaari, H., Portin, H., Teinilä, K., Aurela, M., Dal Maso, M., Rönkkö, T., Petäjä, T., and Paasonen, P.: Measurement report: The influence of traffic and new particle formation on the size distribution of 1–800\,nm particles in Helsinki – a street canyon and an urban background station comparison, Atmospheric Chem. Phys., 21, 9931–9953, https://doi.org/10.5194/acp-21-9931-2021, 2021.

Olin, M., Kuuluvainen, H., Aurela, M., Kalliokoski, J., Kuittinen, N., Isotalo, M., Timonen, H. J., Niemi, J. V., Rönkkö, T., and Dal Maso, M.: Traffic-originated nanocluster emission exceeds \chemH_2SO_4-driven photochemical new particle formation in an urban area, Atmospheric Chem. Phys., 20, 1–13, https://doi.org/10.5194/acp-20-1-2020, 2020.

Onasch, T. B., Trimborn, A., Fortner, E. C., Jayne, J. T., Kok, G. L., Williams, L. R., Davidovits, P., and Worsnop, D. R.: Soot Particle Aerosol Mass Spectrometer: Development, Validation, and Initial Application, Aerosol Sci. Technol., 46, 804–817, https://doi.org/10.1080/02786826.2012.663948, 2012.

Paatero, P.: The Multilinear Engine—A Table-Driven, Least Squares Program for Solving Multilinear Problems, Including the n-Way Parallel Factor Analysis Model, J. Comput. Graph. Stat., 8, 854–888, https://doi.org/10.1080/10618600.1999.10474853, 1999.

Petzold, A. and Schönlinner, M.: Multi-angle absorption photometry—a new method for the measurement of aerosol light absorption and atmospheric black carbon, J. Aerosol Sci., 35, 421–441, https://doi.org/10.1016/j.jaerosci.2003.09.005, 2004.

Pirjola, L., Niemi, J. V., Saarikoski, S., Aurela, M., Enroth, J., Carbone, S., Saarnio, K., Kuuluvainen, H., Kousa, A., Rönkkö, T., and Hillamo, R.: Physical and chemical characterization of urban winter-time aerosols by mobile measurements in Helsinki, Finland, Atmos. Environ., 158, 60–75, https://doi.org/10.1016/j.atmosenv.2017.03.028, 2017.

Praplan, A. P., Pfannerstill, E. Y., Williams, J., and Hellén, H.: OH reactivity of the urban air in Helsinki, Finland, during winter, Atmos. Environ., 169, 150–161, https://doi.org/10.1016/j.atmosenv.2017.09.013, 2017.

Rolph, G., Stein, A., and Stunder, B.: Real-time Environmental Applications and Display sYstem: READY, Environ. Model. Softw., 95, 210–228, https://doi.org/10.1016/j.envsoft.2017.06.025, 2017.

Rönkkö, T., Kuuluvainen, H., Karjalainen, P., Keskinen, J., Hillamo, R., Niemi, J. V., Pirjola, L., Timonen, H. J., Saarikoski, S., Saukko, E., Järvinen, A., Silvennoinen, H., Rostedt, A., Olin, M., Yli-Ojanperä, J., Nousiainen, P., Kousa, A., and Dal Maso, M.: Traffic is a major source of atmospheric nanocluster aerosol, Proc. Natl. Acad. Sci., 114, 7549–7554, https://doi.org/10.1073/pnas.1700830114, 2017.

Rönkkö, T., Pirjola, L., Karjalainen, P., Simonen, P., Teinilä, K., Bloss, M., Salo, L., Datta, A., Lal, B., Hooda, R. K., Saarikoski, S., and Timonen, H.: Exhaust particle number and composition for diesel and gasoline passenger cars under transient driving conditions: Real-world emissions down to 1.5 nm, Environ. Pollut., 338, 122645, https://doi.org/10.1016/j.envpol.2023.122645, 2023a.

https://doi.org/10.5194/egusphere-2024-2235
Preprint. Discussion started: 7 October 2024

Rönkkö, T., Saarikoski, S., Kuittinen, N., Karjalainen, P., Keskinen, H., Järvinen, A., Mylläri, F., Aakko-Saksa, P., and Timonen, H.: Review of black carbon emission factors from different anthropogenic sources, Environ. Res. Lett., 18, 033004, https://doi.org/10.1088/1748-9326/acbb1b, 2023b.

Saarikoski, S., Timonen, H., Saarnio, K., Aurela, M., Järvi, L., Keronen, P., Kerminen, V.-M., and Hillamo, R.: Sources of organic carbon in fine particulate matter in northern European urban air, Atmospheric Chem. Phys., 8, 6281–6295, https://doi.org/10.5194/acp-8-6281-2008, 2008.

Savadkoohi, M., Pandolfi, M., Reche, C., Niemi, J. V., Mooibroek, D., Titos, G., Green, D. C., Tremper, A. H., Hueglin, C., Liakakou, E., Mihalopoulos, N., Stavroulas, I., Artiñano, B., Coz, E., Alados-Arboledas, L., Beddows, D., Riffault, V., De Brito, J. F., Bastian, S., Baudic, A., Colombi, C., Costabile, F., Chazeau, B., Marchand, N., Gómez-Amo, J. L., Estellés, V., Matos, V., van der Gaag, E., Gille, G., Luoma, K., Manninen, H. E., Norman, M., Silvergren, S., Petit, J.-E., Putaud, J.-P., Rattigan, O. V., Timonen, H., Tuch, T., Merkel, M., Weinhold, K., Vratolis, S., Vasilescu, J., Favez, O., Harrison, R. M., Laj, P., Wiedensohler, A., Hopke, P. K., Petäjä, T., Alastuey, A., and Querol, X.: The variability of mass concentrations and source apportionment analysis of equivalent black carbon across urban Europe, Environ. Int., 178, 108081, https://doi.org/10.1016/j.envint.2023.108081, 2023.

Schraufnagel, D. E.: The health effects of ultrafine particles, Exp. Mol. Med., 52, 311–317, https://doi.org/10.1038/s12276-020-0403-3, 2020.

Stein, A. F., Draxler, R. R., Rolph, G. D., Stunder, B. J. B., Cohen, M. D., and Ngan, F.: NOAA's HYSPLIT Atmospheric Transport and Dispersion Modeling System, Bull. Am. Meteorol. Soc., 96, 2059–2077, https://doi.org/10.1175/BAMS-D-14-00110.1, 2015.

Steinemann, A.: Volatile emissions from common consumer products, Air Qual. Atmosphere Health, 8, 273–281, https://doi.org/10.1007/s11869-015-0327-6, 2015.

Teinilä, 2024. DOI 10.5281/zenodo.13254916.

Teinilä, K., Timonen, H., Aurela, M., Kuula, J., Rönkkö, T., Hellèn, H., Loukkola, K., Kousa, A., Niemi, J. V., and Saarikoski, S.: Characterization of particle sources and comparison of different particle metrics in an urban detached housing area, Finland, Atmos. Environ., 272, 118939, https://doi.org/10.1016/j.atmosenv.2022.118939, 2022.

Teinilä, K., Aurela, M., Niemi, J. V., Kousa, A., Petäjä, T., Järvi, L., Hillamo, R., Kangas, L., Saarikoski, S., and Timonen, H.: Concentration variation of gaseous and particulate pollutants in the Helsinki city centre — observations from a two-year campaign from 2013–2015, 24, n.d.

Trechera, P., Garcia-Marlès, M., Liu, X., Reche, C., Pérez, N., Savadkoohi, M., Beddows, D., Salma, I., Vörösmarty, M., Casans, A., Casquero-Vera, J. A., Hueglin, C., Marchand, N., Chazeau, B., Gille, G., Kalkavouras, P., Mihalopoulos, N., Ondracek, J., Zikova, N., Niemi, J. V., Manninen, H. E., Green, D. C., Tremper, A. H., Norman, M., Vratolis, S., Eleftheriadis, K., Gómez-Moreno, F. J., Alonso-Blanco, E., Gerwig, H., Wiedensohler, A., Weinhold, K., Merkel, M., Bastian, S., Petit, J.-E., Favez, O., Crumeyrolle, S., Ferlay, N., Martins Dos Santos, S., Putaud, J.-P., Timonen, H., Lampilahti, J., Asbach, C., Wolf, C., Kaminski, H., Altug, H., Hoffmann, B., Rich, D. Q., Pandolfi, M., Harrison, R. M., Hopke, P. K., Petäjä, T., Alastuey, A., and Querol, X.: Phenomenology of ultrafine particle concentrations and size distribution across urban Europe, Environ. Int., 172, 107744, https://doi.org/10.1016/j.envint.2023.107744, 2023.

Vanhanen, J., Mikkilä, J., Lehtipalo, K., Sipilä, M., Manninen, H. E., Siivola, E., Petäjä, T., and Kulmala, M.: Particle Size Magnifier for Nano-CN Detection, Aerosol Sci. Technol., 45, 533–542, https://doi.org/10.1080/02786826.2010.547889, 2011.

Vanhanen, J., Svedberg, M., and Miettinen, E.: Dekati Diluter characterization in the 1-20 nm particle size range, n.d.

Vestenius, M., Leppänen, S., Anttila, P., Kyllönen, K., Hatakka, J., Hellén, H., Hyvärinen, A.-P., and Hakola, H.: Background concentrations and source apportionment of polycyclic aromatic hydrocarbons in south-eastern Finland, Atmos. Environ., 45, 3391–3399, https://doi.org/10.1016/j.atmosenv.2011.03.050, 2011.

Wu, D., Fei, L., Zhang, Z., Zhang, Y., Li, Y., Chan, C., Wang, X., Cen, C., Li, P., and Yu, L.: Environmental and Health Impacts of the Change in NMHCs Caused by the Usage of Clean Alternative Fuels for Vehicles, Aerosol Air Qual. Res., 20, 930–943, https://doi.org/10.4209/aaqr.2019.09.0459, 2020.

https://doi.org/10.5194/egusphere-2024-2235
Preprint. Discussion started: 7 October 2024

955 Zanobetti, A., Austin, E., Coull, B. A., Schwartz, J., and Koutrakis, P.: Health effects of multi-pollutant profiles,
956 Environ. Int., 71, 13–19, https://doi.org/10.1016/j.envint.2014.05.023, 2014.